Environmental Science and Pollution Research (2022) 29:69652–69679
https://doi.org/10.1007/s11356-022-20607-1

RESEARCH ARTICLE

Factors driving sediment compositional change in the distal area of the Ria de Vigo (NW Spain): oceanographic processes vs. paleopollution

Maria Virginia Alves Martins[1,2] · Lucas Cazelli[1] · Missilene Yhasnara[1] · Layla da CristineSilva[1] · Murilo Barros Saibro[1] · Fabia Emanuela Rafaloski Bobco[3] · Belen Rubio[4] · Bruna Ferreira[2] · Wellen Fernanda Louzada Castelo[1] · José Francisco Santos[2] · Sara Ribeiro[2] · Fabrizio Frontalini[5] · Michael Martínez-Colón[6] · Egberto Pereira[1] · Luzia Antonioli[1] · Mauro Geraldes[1] · Fernando Rocha[2] · Silvia Helena Mello e Sousa[7] · João Manuel Alveirinho Dias[8]

Received: 14 October 2021 / Accepted: 29 April 2022 / Published online: 16 May 2022

Abstract

We analyze potential Late Holocene metal contamination along a sediment core collected in the distal zone of Ria de Vigo (North Spain). Statistical treatment of the dataset based on a multiproxy approach enabled us to identify and disentangle factors influencing the depositional processes and the preservation of the records of this activity in the area over the last ≈3000 years BP. Some layers of the analyzed core have significant enrichment in Cu and a moderate enrichment in Ag, Mo, As, Sb, S, Zn, Ni, Sn, Cd, Cr, Co, Pb, and Li. The enrichment of these elements in some layers of this core may be related to mining activities that have taken place since classical times in the region. Successive phases of pollution were identified along the core KSGX24 related to the Late Bronze Age (≈3000–2450 years BP), Iron Age (≈2450–1850 years BP), Roman times (≈1850–1550 years BP), Middle Ages (≈1250–500 years BP), and industrial and modern (≈250–0 years BP) anthropic activities. The protection of the Cies Islands, the erosive and transport capacity of the rivers in the region, oscillations of the oceanographic and climatic regime, atmospheric contamination, and diagenetic sedimentary processes might have contributed to the accumulation and preservation of this record in the distal region of the Ria de Vigo. The studied core shows that the industrial and preindustrial anthropic impacts caused an environmental liability and contributed to the presence of moderate to heavy pollution of various metals in surface and subsurface sediment layers in the distal sector of the Ria de Vigo, which could be a hazard to biota.

Keywords Paleopollution · Trace elements · Sediments · Benthic foraminifera · Stable isotopes · Coastal area · Late Holocene

Responsible Editor: V.V.S.S. Sarma

✉ Maria Virginia Alves Martins
virginia.martins@ua.pt

[1] Faculdade de Geologia, Universidade Do Estado Do Rio de Janeiro, UERJ, Av. São Francisco Xavier, 24, sala 2020A, Maracanã, Rio de Janeiro, RJ 20550-013, Brazil

[2] GeoBioTec, Departamento de Geociências, Universidade de Aveiro, Campus de Santiago, 3810-193 Aveiro, Portugal

[3] Universidade Federal Do Rio de Janeiro (UFRJ), Instituto de Geociências (Igeo) Av. Athos da Silveira Ramos, Bloco G, Cidade. Universitária, Ilha Do Fundão, Rio de Janeiro, RJ 274, Brazil

[4] Departamento de Xeociencias Mariñas E Ordenación Do Territorio, Universidade de Vigo, Edificio de Ciencias Experimentais Campus de Vigo, 36310 Vigo, Spain

[5] Department of Pure and Applied Sciences, Università Degli Studi Di Urbino "Carlo Bo", 61029 Urbino, Italy

[6] School of the Environment, FSH Science Research Center, Florida A and M University, 1515 South MLK Blvd, Tallahassee, FLFL USA 32307, USA

[7] Instituto Oceanográfico, Universidade de São Paulo, Praça Do Oceanográfico, São Paulo, SP 191, Brazil

[8] Centro de Investigação Marinha E Ambiental (CIMA), Universidade Do Algarve, Campus de Gambelas, Faro, Portugal

Introduction

Anthropic activities have promoted and intensified atmosphere, oceans, and biosphere changes. Global human disturbances have led stratigraphers to recognize the existence of a new "stage," still under debate, the Anthropocene (Zalasiewicz et al. 2011). Many pollution studies have focused on the current or post-industrial period in densely populated and heavily industrialized coastal areas that have often resulted in environmental degradation and the imbalance of natural ecosystems (Bardos et al. 2020; Rahman et al. 2021). However, the records and effects of preindustrial anthropic impact on these regions are much less studied, particularly regarding mining, for example. Mining activities, closely linked to the exploitation of natural resources, have occurred in several regions of the world since classical times (Radivojević et al. 2019). In South Iberia, for instance, pollution from anthropogenic sources caused by the mining of metal sulfide ores has occurred since at least 3250–3000 BCE (the Copper Age; Emslie et al. 2015, 2019; Leblanc et al. 2000; Rovira 2002). By that time, northern Iberian communities had undergone a crucial historical trajectory regarding mining activity (e.g., de Blas 1996, 2005; Martínez-Cortizas et al. 2002, 2012, 2016). In Roman times (AD 1st to fourth centuries), the significant mining resources available, including lead, silver, gold, and copper, made the Iberian Peninsula the first district to be exploited on a large scale (Claude 1987; Comendador Rey et al. 2016; Orejas and Sánchez-Palencia 2002; Penhallurick 1986). The record of these activities is well marked, for example, in peat bogs of the NW Iberian Peninsula (e.g., Kylander et al. 2005; Martínez Cortizas et al., 1997b, 1999; Olid et al. 2010; Pontevedra-Pombal et al. 2013; Rodríguez-Racedo et al. 2013). Records show that contemporaneous pollution resulting from some anthropogenic activities, in particular mining and metallurgy, has already caused negative effects on local populations, for example, low to chronic doses of mercury and lead exposure (Álvarez-Fernandez et al. 2020; López-Costas et al. 2020).

Recently, concerns about environmental degradation in the Galician Rias have led to several studies on pollution in surface sediments (e.g., Barreiro Lozano et al. 1988; Canário et al. 2007; Carballeira et al. 1997; Carral et al. 1995a, 1995b; Pérez-López et al. 2004; Rubio et al. 2000) and sediment cores (e.g., Álvarez-Vázquez et al. 2020; Rubio et al. 2010). Some authors have analyzed diagenetic processes that favored the retention and mobilization of metals, increasing the risk of sediment toxicity (e.g., Álvarez-Iglesias and Rubio 2008, 2009; Belzunce Segarra et al. 2008; Andrade et al. 2011; Ramírez-Pérez et al. 2020; Rubio et al. 2010).

The Ria de Vigo region has also been the target of several geological, oceanographic, and paleoenvironmental reconstitutions (e.g., Diz et al. 2002; González Álvarez et al. 2005; Martins et al. 2013a; Méndez and Vilas 2005). Méndez and Vilas (2005) inferred that between 3000 and 700 years BP, dominance in the estuarine circulation of the Rias Baixas might have occurred as well as an increase in the exchange of water between these rias and the ocean since about 500 years BP. González Álvarez et al. (2005) also noticed a significant environmental change that took place at 2850 years cal BP, in the transition between the Subboreal/Sub-Atlantic climates, marked by high storminess in the mid-latitudes. Diz et al. (2002), González Álvarez et al. (2005), and Martins et al. (2007, 2013a) identified reinforced upwelling pulses in the region around ≈2200–1200 years calibrated before present (cal BP) and in the past ≈500 years cal BP.

Although many studies on recent sediment pollution have been conducted in the Galician Rias Baixas in the last decades (e.g., Álvarez-Vázquez et al. 2020; Barreiro Lozano et al. 1988; Canário et al. 2007; Carballeira et al. 1997; Carral et al. 1995a, 1995b; Pérez-López et al. 2004; Prego and Cobelo-Garcia 2003; Rubio et al. 2000, 2010), to our knowledge, only the works of López Costas et al. (2020) and Álvarez-Iglesias et al. (2020) has analyzed paleopollution (before the industrial revolution). The research presented in both works was performed on human remains of the archaeological settlement of A Lanzada, which is located in the outer, northern sector of the Ría de Pontevedra and analyzed the effects of atmospheric mercury and lead exposure at the edge of the Roman World. However, no work of this nature has yet been done in the Ria de Vigo, particularly studies using marine sediment cores.

In this context, the present work analyzes the possible record of paleopollution in the last ≈3000 years BP by Ag, As, Cd, Co, Cr, Cu, Ni, Pb, Sb, Sn, and Zn, which is related to several phases of mining activity that have occurred in the region. This record was obtained in a sediment core from the distal sector of Ria de Vigo (Spain), which is protected by the Cies Islands (Fig. 1). This study also associates the metal pollutants with possible lithological sources received in the study area as well as the atmospheric contribution divulged in the literature (Kylander et al. 2005; López-Merino et al. 2014; Martínez-Cortizas et al. 1997a, 2005, 2012, 2013, 2016; Olid et al. 2010, 2013; Pontevedra-Pombal et al. 2013). The probable influence of changes in oceanographic and climatic regimes and the factors that may have allowed the preservation of the paleopollution record in the study sediments were also analyzed.

Study area

The rias of Galicia (NW of the Iberian Peninsula) are a set of elongated coastal inlets that are fault-bounded embayments spreading over 1720 km of the Iberian coast (Méndez and Vilas 2005; Vilas et al. 2019). The Ria de Vigo (172 km^2) is the southernmost of these rias and is characterized by a funnel shape, with depths in its central axes of the

outer zone of approximately 40–60 m and in the inner zone of 5–10 m.

Ria de Vigo lies in the Iberian Variscan orogenic domain, formed during the Paleozoic (Julivert et al. 1980; Martínez Catalán et al. 2019) in the Galicia-Trás-os-Montes Zone (GTMZ; Fig. 1; Farias et al. 2014). The GTMZ represents a stack of parautochthonous and allochthonous units (or Schistose Domain; Farias et al. 2014) thrust over the autochthonous Central Iberian Zone (represented by the Ollo de Sapo formation) during the Variscan orogeny (Fig. 1; Llera et al. 2019; Ribeiro et al. 1990). The allochthonous units comprise metasediments and metavolcanics, as well as orthogneisses—an ophiolitic unit and an upper allochthonous unit—which includes a variety of rocks affected by granulite and eclogite facies metamorphism as well as abundant ultramafic lithologies (Fig. 1; e.g., Díez Fernández et al. 2012; Iglésias et al. 1983; Ribeiro et al. 1990; Rodrigues et al. 2013).

The Galiñeiro igneous complex, which crosses the Ria de Vigo, is composed of peralkaline magmas (Montero et al. 2009), including aegirine-riebeckite orthogneisses. The complex has high concentrations of high-field-strength elements such as Zr, Hf, Nb, Ta, and Th, as well as rare earth elements (REE; Floor 1966; Montero et al. 2009). Some pegmatite bodies that intruded the allochthonous metasedimentary sequences of the Schistose Domain (Llera et al. 2019) are characterized by the presence of Li–Sn–Ta mineralizations (Canosa et al. 2012; Fuertes-Fuente et al. 2000). Some mineralized pegmatites are probably genetically related to peraluminous two-mica granites (Fuertes-Fuente and Martin-Izard 1994; Llera et al. 2019). The erosion of these rocks supplied the coastal Quaternary sediments found in the region (García-García et al. 2005).

In the Ria de Vigo, two sectors, namely internal and external, can be recognized according to hydrodynamic and sedimentological characteristics. The external zone, located at the mouth of the ria, is dominated by waves, although it is protected from direct oceanic influence by the Cies Islands, which act as a natural barrier and control oceanic influence and sedimentary processes (Vilas et al. 2019). The internal sector presents an estuarine behavior and is shallower.

Several rivers, such as the Verdugo-Oitavén and the Lagares (Fig. 1C), flow into the Ria de Vigo, comprising a watershed of 709 km^2. The rivers cross Paleozoic alkaline and calc-alkaline granitic and metamorphic (schist and gneiss) lithologies, showing seasonal variability in their discharge and sediment load (Méndez and Vilas 2005; Pazos et al. 2000; Perez-Arlucea et al. 2005). The Verdugo-Oitavén rivers are the largest and join together before flowing into the San Simón Bay, constituting about 57.3% of the total catchment area and providing a major sediment load to the ria (Méndez and Vilas 2005; Pazos et al. 2000; Perez-Arlucea et al. 2005).

The surface water temperature has a strong seasonal gradient varying between 11 and 12 °C (winter) and 19 and 20 °C (summer). The salinity gradient varies between 36 toward the mouth of the ria and 31–32 toward the river mouths in the San Simón Bay (Nombela et al. 1995). On the ria's coast, waves from 1 to 2.5 m are predominant most of the year, but they can exceed 3 m in height in winter (Chao et al. 2002). Accordingly, the Galician territory has some of the highest winds in the Iberian Peninsula, which may exceed 10 m/s in higher regions (Troen and Petersen 1989).

The wind regime has a considerable influence on the seasonality of oceanographic processes in the region. In spring and summer (mainly from May to September), the prevalence of northerly winds over the oceanic coastal surface results in upwelling events (Fiúza 1983; Fiúza et al. 1982; Wooster et al. 1976). During the rainy season (usually from October to April), greater amounts of fluvial sediments are introduced into the marine system. These seasonal variations, coupled with downwelling regimes and the development of currents toward the poles, result in the hydrodynamic transfer of resuspended materials to the north and offshore (Jouanneau et al. 2002; Martins et al. 2007; Torres and Barton 2007). By analyzing the sediments of transitional coastal systems such as the Galician rias, it is possible to recognize periods of higher terrestrial vs. marine influence related to the seasonality of fluvial-derived sediment plumes and oceanographic processes (Bernárdez et al. 2008). These seasonal factors can play an important role in the fate and transport of pollutants from polluted areas near the continent.

Materials and methods

A core KSGX24 (236 cm long) was collected in July 1998 on the GAMINEX oceanographic cruise in the external sector of the Ria de Vigo near the Cies Islands (42°12′48″N, 8°51′90″W at a water depth of 39 m; Fig. 1). The research was conducted on the Galician and Northern Portuguese border in collaboration with the Hydrographic Institute of Portugal and the University of Algarve under the Ocean Margin Exchange Project (OMEX). The core was sampled at every 1-cm interval (e.g., 0–1 cm, 2–3 cm, 4–5 cm, etc.) along its entire length.

Sediment texture

The sediment texture was analyzed by Martins et al. (2013a) with a laser diffraction particle size analyzer (Malvern Master Size) after the elimination of organic matter and carbonates with oxygen peroxide and hydrochloric acid, respectively. The percentage of fine silt + clay (< 15 μm), medium silt (15–30 μm), coarse silt (30–63 μm), very fine sand (63–125 μm), fine sand (125–250 μm), medium sand (250–500 μm), and coarse sand (> 500 μm) were determined,

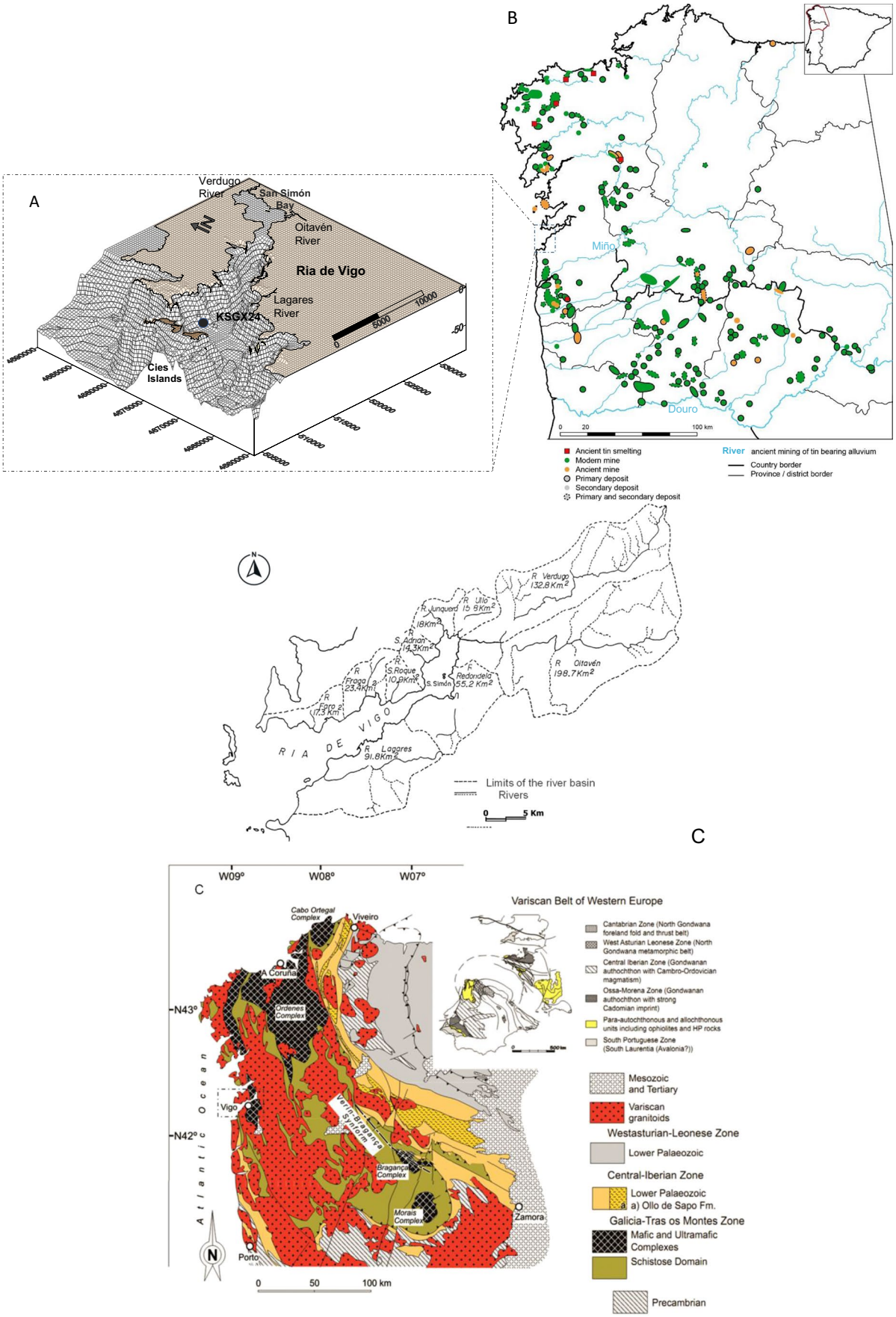
A
Verdugo River
San Simón Bay
Oitavén River
Ria de Vigo
Lagares River
KSGX24
Cies Islands
B
Miño
Douro
0 20 100 km
Ancient tin smelting
Modern mine
Ancient mine
Primary deposit
Secondary deposit
Primary and secondary deposit
River ancient mining of tin bearing alluvium
Country border
Province / district border
R Verdugo 132.8Km2
R Junquera 18Km2
R Ulló 15.8Km2
R S.Adrian 19.3Km2
R S.Roque 10.9Km2
R Froga 23.4Km2
R Redondela 55.2 Km2
S.Simón
R Oitavén 198.7Km2
R Lagares 91.8Km2
RIA DE VIGO
Limits of the river basin
Rivers
0 5 Km
C
W09°
W08°
W07°
N43°
N42°
Cabo Ortegal Complex
Viveiro
A Coruña
Ordenes Complex
Vigo
Verin-Braganza Synform
Bragança Complex
Morais Complex
Zamora
Porto
Atlantic Ocean
0 50 100 km
Variscan Belt of Western Europe
Cantabrian Zone (North Gondwana foreland fold and thrust belt)
West Asturian Leonese Zone (North Gondwana metamorphic belt)
Central Iberian Zone (Gondwanan authochthon with Cambro-Ordovician magmatism)
Ossa-Morena Zone (Gondwanan authochthon with strong Cadomian imprint)
Para-autochthonous and allochthonous units including ophiolites and HP rocks
South Portuguese Zone (South Laurentia (Avalonia?))
Mesozoic and Tertiary
Variscan granitoids
Westasturian-Leonese Zone
Lower Palaeozoic
Central-Iberian Zone
Lower Palaeozoic
a) Ollo de Sapo Fm.
Galicia-Tras os Montes Zone
Mafic and Ultramafic Complexes
Schistose Domain
Precambrian

◂**Fig. 1** **A** Bathymetric map, some rivers, and the location of the KSGX 24 core in the Ria de Vigo. **B** Tin exploitation sites in the northwestern Peninsula (Meunier 2011). **C** Main rivers (R) that flow into the Ria de Vigo (adapted from Vilas et al. 1995). **D** Geological sketch of the NW Iberian Peninsula (adapted from Farias et al. 2014)

as well as textural parameters such as sediment mean grain size (SMGS), sorting and skewness, according to Folk and Ward (1957).

Geochemical data

The concentration of elements (except Si) was determined in a fine fraction (< 63 μm) after digestion with four acids ($HClO_4$, HNO_3, HCl, HF) and determined by inductively coupled plasma-mass spectrometry analysis at ACME Laboratory (Canada). Detection limits for each element (> 95% accuracy) are listed in Appendix 1. Silicon (Si) concentrations were determined in 40 samples by atomic absorption spectrophotometry based on dissolved sediments with three-acid decomposition, $HCl + HNO_3 + HF$. This work includes elemental concentrations analyzed by Martins et al. (2013a, b, 2016) along with the core (Al, As, Ca, Ce, Co, Cr, Fe, Ga, K, La, Li, Ni, S, Sc, Sr, Th, V, and Zn) and also new other elements (original data), such as Ag, Ba, Be, Cd, Cs, Cu, Dy, Er, Eu, Gd, Hf, Ho, Lu, Mg, Mn, Mo, Na, Nd, P, Pb, Pr, Rb, Sb, Si, Sm, Sn, Ta, Tb, Ti, Tm, U, V, W, Y, Yb, and Zr, as well as $\delta^{13}C$, $\delta^{15}N$, Nd, and Sr isotopic data.

The $\delta^{13}C$ and $\delta^{15}N$ isotopic data were analyzed in organic matter using a Thermo Finnigan MAT253 mass spectrometer at the University of Vigo. Isotopic values refer to the V-PDB pattern. Total organic carbon (TOC) for the first 39 cm of the core was analyzed by combustion in a LECO CS Analyzer 125 (Martins et al. 2013a). After carbonate removal, neodymium and strontium isotopes were analyzed in bulk sediment samples from six selected layers along the core using a VG Sector 54 thermal ionization mass spectrometer in the Laboratory of Isotope Geology of Aveiro University according to the methodology described by Ribeiro et al. (2011) and Martins et al. (2013b, 2018).

Geochemical indices

The use of elemental enrichment factors has been increasingly used to estimate the impact caused by pollution, that is, to determine how much the metal concentration in a sample increases in relation to their average value in the environment when anthropogenic action is absent. For determination of the chemical elements, however, it is necessary to have "background" concentrations as a reference (i.e., the concentration of metals in pristine sediment unaffected by human activity; Birch 2017). Several authors have criticized the way background concentrations have been estimated due to several factors such as sediment geochemical analysis procedures, applied statistical methods, the variable composition of the Earth's crust, and different erosion processes from various elements such as climate, the density of the hydrographic network, and regional geomorphological characteristics (Bern et al. 2019; Carranza 2017; Reimann and De Caritat 2000).

According to Birch (2017), the most widely used procedures are the use of world shale (e.g., Turekian and Wedepohl 1961), pristine marine and fluvial sediments, and catchment soils and rocks, with the use of sedimentary cores being the method that presents the greatest advantage. Considering the great utility of the analysis of the metal enrichment in relation to background values, this methodology was applied in this work. Some authors have proposed values for several chemical elements (e.g., Álvarez-Iglesias et al. 2006; Rubio et al. 2000), but the database does not include all the chemical elements analyzed in this paper. No studies in Ria de Vigo or the region contain background values for all the chemical elements used in this work. Therefore, considering the various analytical methodologies applied in this study, this work used as background values the mean elemental concentrations of 12 samples of core KSGX40 (original data from this work) from sediment layers deposited prior to 4000 years BP (according to Martins et al. 2007). Core KSGX40 was collected on the adjacent continental shelf (in the Galicia Mud Deposit, off the Ria de Vigo, at latitude 42°14′98″N, longitude 09°01′01″W, at a sea depth of 115 m) and subjected to the same methodology of analysis, also in the ACME Laboratory (Canada). These data were selected as they are local values of unpolluted marine sediments related to regional lithologies from a muddy deposit with similar characteristics to the analyzed core.

The enrichment factors (EF) of the analyzed chemical elements were calculated based on the equation (Buat-Menard and Chesselet 1979):

$$\mathrm{EF} = \frac{\left(\frac{Cx}{Cn}\right)\text{Environment}}{\left(\frac{Cx}{Cn}\right)\text{Baseline}}$$

where Cx is the concentration of the element x whose enrichment is to be determined and Cn is the concentration of the normalizing element n. In this work. Al was used as a normalizer, as it is a conservative lithogenic chemical element associated with fine-grained sediments, namely clay minerals (Windom et al. 1989), and is considered adequate to remove the influence of metal enrichment in this region, as analyzed by Rubio et al. (2000). The classification of the EF values was based on Sutherland (2000), as follows: EF < 2, null or minimal contamination; 2 > EF < 5, moderate enrichment; 5 > EF < 20, significant enrichment; 20 > EF < 40, very high enrichment, indicating a high level

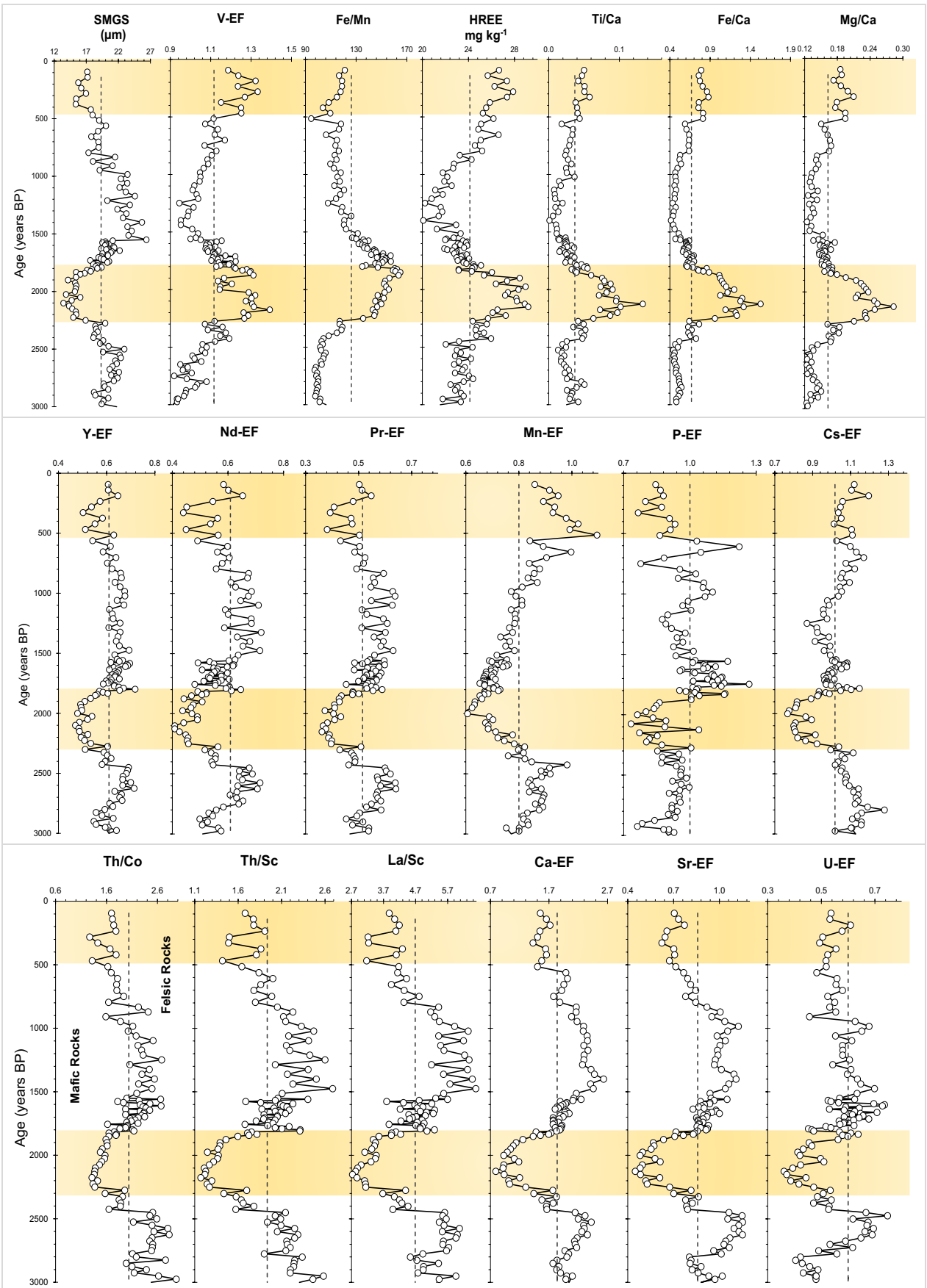
SMGS (μm)
V-EF
Fe/Mn
HREE mg kg-1
Ti/Ca
Fe/Ca
Mg/Ca
Y-EF
Nd-EF
Pr-EF
Mn-EF
P-EF
Cs-EF
Th/Co
Th/Sc
La/Sc
Ca-EF
Sr-EF
U-EF
Age (years BP)
Mafic Rocks
Felsic Rocks

◂**Fig. 2** Age plots of the values of sediment mean grain size (SMGS; μm), enrichment factors (EF) of several chemical elements, heavy rare earth elements (HREE) concentrations (mg kg^{-1}), and the ratios Fe/Mn, Ti/Ca, Fe/Ca, Mg/Ca, Th/Co, Th/Sc, and La/Sc. The mean value of each variable (dashed vertical line) is shown. The finest sediment sections are are shaded

of contamination; and EF > 40, extremely high enrichment, indicating extreme contamination.

The Igeo was calculated according to Müller (1986):

$$\text{Igeo} = \log_2\left[\frac{\text{Cx}}{\text{Cbx1.5}}\right]$$

where *Cx* is the concentration of the metal ("*x*") in the sediment layer and *Cb* is the corresponding baseline concentration (Appendix 2). The Igeo values were used to identify polluted sediments and classified as follows (Müller 1986): <0, unpolluted; 0–1, unpolluted to moderately polluted; 1–2, moderately polluted; 2–3, moderately to strongly polluted; 3–4, strongly polluted; 4–5, strongly to extremely polluted; and >5, extremely polluted.

Benthic foraminifera

The database of benthic foraminifera from Martins et al. (2013a) was improved: aged and transported specimens (whose abundance is significant along the KSGX24 core) were removed from the previous count. Specimen counts (in the sediment fraction > 63 μm) were increased until ideally reaching a number of at least 300 specimens per sample (*N* between 292–850; mean 511 ± 117); the percentage of the species per sample was recalculated. Foraminiferal density provides information on the abundance of specimens: FD = number of specimens/g of bulk sediment. The percentage of species that are more frequent in the middle-outer shelf (MOS) than in coastal transitional areas (Martins et al. 2012, 2019) was calculated to trace higher marine influence in the distal region of the Ria de Vigo. The density (number per gram of total sediment) of planktonic foraminifera and biogenic particles such as sea urchin spikes, fragments and spikes of sponges, bryozoan remains, and pyritized foraminifera were also determined (new data of this work).

Age model

Ages taken from Martins et al. (2013a) have been reinterpreted in this work. These authors obtained radiocarbon ages at Beta Analytic, Inc. (Miami, FL, USA, by accelerator mass spectrometry (AMS)) for the sediment layers (33–34 cm, 71–72 cm, 143–144 cm, and 193–194 cm; Appendix 3) using *Cibicides* spp. (foraminiferal) samples (10 to 20 mg, with size > 125 μm). Radiocarbon ages were calibrated (2σ calibration) using the OxCal v4.1.7 program (Bronk Ramsey 2001, 2008, 2009, 2010). For this work, the radiocarbon ages were corrected for the reservoir effects estimated by Soares and Dias (2007). Intermediate ages were estimated by interpolation (Appendix 3).

Statistical analysis

Before statistical analyses, data were log-transformed (log $x+1$). Pearson correlations were performed with a recognized level of significance of $p < 0.05$. Relationships among the analyzed variables were explored through two principal component analyses (PCA) based on Pearson correlation matrices between (A) concentrations and (B) EF of chemical elements and other geochemical, textural, and biotic variables. These analyses were performed using the TIBCO Statistica® 13.5.0 software.

Foraminiferal ecological parameters (i.e., species richness (SR); Shannon diversity, Shannon 1948 (*H′*) and equitability, Magurran 1988 (*J′*)) were calculated in Primer 6. A bathymetric map with the location of the studied core was performed in Surfer software 14. The mean values and the moving average, determined with three successive data along the core, were applied to some graphs to identify general trends.

Results

Sedimentological results

The results analyzed in this work are included in Appendices 1, 2, 3, 4, 5, 6, 7, and 8. The age model based on the radiocarbon ages indicates that the KSGX24 core records the last ≈3000 years BP (Appendix 3). This core is composed essentially of fine-grained sediments (fine fraction, < 63 μm, ranging from 76.30 to 92.84%; mean 84.41 ± 3.37%) with sediment mean grain size (SMGS) values varying from 9.07 to 26.36 μm (mean 19.34 ± 2.85 μm; Fig. 2; Appendix 4). The range of the elemental concentrations and the baseline concentrations used in this work are presented in Appendix 2. The highest concentrations of major elements, in decreasing order, were found for Si, Al, Ca, Fe, K, S, Na, Mg, Ti, and P (Appendices 1 and 2). The trace elements that reached concentrations > 20 mg kg^{-1} are, in decreasing order, Ba, Sr, Mn, Rb, Zr, Li, Ag, Zn, Ce, V, Cr, Cu, La, Ni, Nd, Pb, and As (Appendices 1 and 2). In some layers of the core, certain elements attain concentrations higher than the background values. In some layers, the enrichment factors (EF; Appendix 1) reached values between 5 and 20 for Cu

and between 2 and 5 for Ag, Mo, As, Sb, Zn, Ca, S, Ni, Sn, Cd, Cr, Co, Pb, and Li. The other elements have EF < 2.

Some geochemical variables tended to present an opposite distribution pattern to SMGS, reaching higher values in the finer sections of the sediments, such as V-EF, Fe/Mn, heavy REE (HREE), Ti/Ca, Fe/Ca, and Mg/Ca (Fig. 2). Others show a marked reduction or tend to decline in the finer sections of the sediments, for example, Y-EF, Nd-EF, Pr-EF, Mn-EF, P-EF, Cs-EF, Ca-EF, Sr-EF, and U-EF, as well as Th/Co, Th/Sc, and La/Sc (Fig. 2).

Based on the geochemical and grain size data, it is possible to identify several intervals along the KSGX40 core.

Phase 1, ≈3000–2450 years BP, marked by peaks of Cd-EF, Cr-EF, Ni-EF, and Sn-EF associated with relatively coarser sediments and relatively high Ca-EF, Cs-EF, Mn-EF, Mo-EF, Nb-EF, Pr-EF, Sr-EF, and Ta-EF and/or Li-EF, V-EF, Y-EF, Th/Co, Th/Sc, and La/Sc values;
Phase 2, ≈2450–1850 years BP, indicated by a sharp increase of As-EF, S-EF, and Sb-EF, as well as peaks of Co-EF, Cr-EF, Cu-EF, Ni-EF, Pb-EF, Sn-EF, and Zn-EF associated with the increase of V-EF, Fe/Mn, HREE, Ti/Ca, Fe/Ca, and Mg/Ca, and decreasing SMGS, Ca-EF, Cs-EF, Mn-EF, Nd-EF, P-EF, Pr-EF, Sr-EF, U-EF, Y-EF, Th/Co, Th/La, and La/Sc;
Phase 3, ≈1850–1550 years BP, showing peaks of Ag-EF, Co-EF, Cr-EF, Li-EF, Mo-EF, P-EF, Pb-EF, Sn-EF, Ta-EF, W-EF, and Zn-EF were observed, associated with the increase or relatively high values of SMGS, Ca-EF, Cs-EF, Mn-EF, Nd-EF, Pr-EF, Sr-EF, U-EF, Y-EF, Th/Co, and La/Sc;
Phase 4, ≈1250–500 years BP, with marked peaks of Cu-EF as well as As-EF, Cd-EF, Cr-EF, Co-EF, Ni-EF, P-EF, and Sn-EF. This phase is also characterized by a decreasing trend of SMGS, Ca-EF, Sr-EF, Th/Co, Th/Sc, and La/Sc values and increasing trends of Cs-EF, Mn-EF, U-EF, and HREE values yet with low values of Fe/Mn, Ti/Ca, Fe/Ca, and Mg/Ca;
Phase 5, from ≈250 years BP, is marked by a sharp increase of Cd-EF, Pb-EF, and W-EF, a rise of Co-EF, Cr-EF, Cu-EF, and Zn-EF, and a decrease of SMGS, Ca-EF Mn-EF, Sr-EF, Th/Co, Th/Sc, and La/Sc.

In some layers or intervals, the Igeo values reached ranges between: 2 and 3 for Cu and As; 1 and 2 for Ag, Sb, Mo, S, Zn, and Ni; and 0 and 1 for Sn, Pb, Cd, V, Co, Cr, Fe, and W (Appendix 1). The age plots of Igeo values for Cu, S, Ag, As, and Sb are presented in Figure S1, which also shows the layers where these values are higher (Fig. 3).

Isotopic data

Values of $^{143}Nd/^{144}Nd$ and $^{87}Sr/^{86}Sr$ are presented as a function of age in Appendix 5. As Sr and Nd isotope data were analyzed after carbonate removal, the results essentially reflect the terrigenous fraction. The values of $^{143}Nd/^{144}Nd$ ranged from 0.511992 to 0.512043 and correspond to a variation of ε_{Nd} between 11.6 and 12.6, putting into evidence a strong homogeneity of the Nd isotope composition (Fig. 4). The values of $^{87}Sr/^{86}Sr$ vary between 0.729791 and 0.732354. The highest $^{87}Sr/^{86}Sr$ values were recorded in the lower part of the core (Appendix 5), but given the limited number of analyzed samples, it is unclear whether that represents a reliable trend. The ε_{Nd} vs. $^{87}Sr/^{86}Sr$ biplot (Fig. 4) reveals that the analyzed samples lie in a small area within the fields of typical compositions of the western European crust.

Values of $\delta^{13}C$ in organic matter varied from − 23.04 to − 24.57‰ (mean − 23.69 ± 0.3‰; Appendix 1). The highest values of $\delta^{13}C$ are recorded in the intervals between ≈2250 and 950 years BP and tend to increase from ≈550 years BP (Fig. 5). Values of $\delta^{15}N$ ranged from 1.85 to 5.84‰ (mean 3.81 ± 0.69‰; Appendix 1).

Benthic foraminifera

The values of FD (82–3300 n/g; mean 912 ± 592 n/g) vary considerably along the core as well as those of SR (25–62, mean 41 ± 7), H' (2.32–3.16; mean 2.77 ± 0.16), and J' (0.63–0.82; mean 0.75 ± 0.03) (Appendix 6). The presence of pyritized foraminifera was observed throughout the entire core (Appendix 6). The abundance of planktonic foraminifera (33 ± 36 n/g) is much smaller than that of benthic foraminifera and presents a pattern identical to the density curve of benthic foraminifera. Other biogenic particles are also observed, such as fossils of foraminifera (old tests), pyritized foraminifera, sea urchin spikes, fragments and spicules of sponges, and bryozoan remains (Appendix 6).

Overall, 198 benthic foraminiferal species and taxa are identified (Appendix 6). The species and taxa that reach ≥ 20% are, in descending order, *Nonion faba* (0–37.5%), *Cibicides* spp. (0.7–35.4%), *Cibicidoides ungerianus* (0–30.8%), *Bolivina pseudoplicata* (2.3–25.9%), *Bolivina ordinaria* (0–21.7%), and *Bolivina spathulata* (0–21.1%; Appendix 6). Some of these species are present along the core but do not show a clear pattern of distribution, such as *Cibicides* spp., *C. ungerianus*, and *B. ordinaria*.

A numerous group of benthic foraminiferal species is more frequent in the MOS environments of the Iberian margin than in coastal transitional areas (Martins et al. 2012, 2019), such as *Bolivina skagerrakensis*, *Bolivina spathulata*, *Bulimina elongata*, *Bulimina marginata*, *Cassidulina laevigata*, *Cassidulina carinata, Nonionella iridea*, *Nonionella stella, Trifarina angulosa*, *Uvigerina* spp., and *Valvulineria bradyana* (complete list in Appendix 6).

The relative abundances of *B. spathulata, V. bradyana* and *N. faba* tend to increase mostly in the middle part of the core (Fig. 5). *Ammonia* species are mainly present at the core base and up to ≈2500 years BP (Fig. 5), and in the central part of the core, only scattered peaks of this species occur.

Statistical results

Pearson correlations and the first two factor loadings (unrotated) of two PCAs relating geochemical, textural, and biogenic variables are presented in Appendices 7 and 8, respectively. The biplots of factor 1 versus factor 2 of the two PCAs relating elemental concentrations and the enrichment factors with other geochemical, textural, and biogenic variables are included in Fig. 5A, B, respectively.

The biplot of factor 1 versus factor 2 of the PCA of Fig. 6A, which explain 69% (factor 1: 54%; factor 2: 15%; Appendix 8), shows that the concentrations of (1) Ca, Ce, Gd, La, Na, Nd, Pr, Rb, Sm, Sr, Th, and Y tend to increase in coarser and sandier sediments and are associated with biotic variables related to foraminiferal density and diversity and abundance of transported foraminifera; (2) Ag, Al, As, Ba, Bi, Co, Cr, Er, Eu, Fe, Ga, Ho, K, Li, Mg, Mo, Ni, P, Pb, S, Sb, Sc, Sr, Tm, U, W, Yb, and Zn are associated with finer-grained sediments and *V. bradyana*, *N. faba*, and *B. spathulata* with MOS and $\delta^{13}C$; (3) Be, Cd, Cs, Mn, Mo, Nb, Sn, Ta, Ti, and Zr are related to *Ammonia* spp. rising; (4) P, Ag, Eu, Lu, Tb, Tm, and U are more related to the increasing remains of bryozoans, sponges, and sea urchins. The concentration of most of the chemical elements has significant correlations (positive or negative) with the fine fraction of the sediments and the relative abundance of *N. faba, V. bradyana, B. spathulata*, and *Ammonia* spp. (Appendix 7).

The biplot of factor 1 versus factor 2, from the PCA in Fig. 6B, which explains 77% (factor 1: 66%; factor 2: 11%), shows that (1) most variables are positively correlated with factor 1, which is associated with coarser and sandier sediments (Ca-EF, Sr-EF, La-EF, Ce-EF, Pr-EF, Th-EF, Y-EF, Rb-EF, Nd-EF, Sm-EF, Zr-EF, Na-EF, Ti-EF, Gd-EF, K-EF, Hf-EF, Mg-EF, Ta-EF, U-EF, Tb-EF, Dy-EF, Nb-EF, Er-EF, Lu-EF, Cs-EF, Yb-EF, Cd-EF, Eu-EF, Mo-EF, Ho-EF, Be-EF, Ba-EF, Sn-EF, P-EF, Mn-EF, W-EF, as well as the ratios La/Sc, Th/Sc, Th/Co), the Shannon index, species richness, density of benthic foraminifera, planktonic foraminifera, and other biogenic remains, such as transported foraminifera and fossil foraminifera; (2) As-EF, Sb-EF, Sc-EF, S-EF, Fe-EF, V-EF, Co-EF, and Pb-EF are related to finer-grained sediments (and the finest fractions), as well as with increased Fe/Ca, Mg/Ca, Ti/Ca, HREE, $\delta^{13}C$, and MOS values and *V. bradyana*, *N. faba*, and *B. spathulata;* (3) biogenic particles, namely foraminiferal density and diversity parameters, are more associated with coarse silt fraction; (4) potentially toxic elements, such as Cr-EF, Ni-EF, Zn-EF, Cu-EF, Pb-EF, W-EF, and Co-EF, and also $\delta^{15}N$, Li-EF, and Ga-EF are negatively related to the foraminifera and other biogenic remains (variables of 3).

Discussion

Tracers of changes in oceanographic processes

Factor 1 of the PCA of Fig. 5A (Appendix 8) and the correlations between the variables (Appendix 7) show that the concentrations of most chemical elements are significantly and positively correlated to finer-grained sediments, MOS and $\delta^{13}C$ values, and several foraminifera species, such as *V. bradyana, N. faba*, and *B. spathulata*, whose frequency typically increases in the mid- to outer-continental shelf (Martins et al. 2019). Since the sediments' grain size is mostly related to hydrodynamic conditions, this means that factor 1 of the PCA of Fig. 6A represents the influence of energy changes, which largely influenced the composition of the sediments.

Note that the enrichment of several chemical elements (e.g., La, Ce, Pr, Th, Y, Rb, Nd, Sm, Zr, Na, Ti, Gd, K, Hf, Mg, Ta, U, Tb, Dy, Nb, Er, Lu, Cs, Yb, Cd, Eu, Mo, Ho, Be, Ba, Sn, P, Mn, W) is associated with coarser sediments, according to the results of the PCA of Fig. 5B (I), which presupposes the prevalence of a more active bottom hydrodynamic regime, different from the one that favored the increase of the variables of the Fig. 5B (II), namely As, S, and Sb. In the region, the hydrodynamics are stronger in autumn and winter, when the rainfall and the SW storms are more intense. These conditions give rise to downwelling events that favor the transport of sediments offshore (Álvarez-Salgado et al. 2000; Jouanneau et al. 2002).

The $\delta^{13}C$ and $\delta^{15}N$ values are proxies widely used for tracing the source of sedimentary organic matter (Barros et al. 2010; Bueno et al. 2019; Martinelli et al. 2009). The biplot of $\delta^{13}C$ against $\delta^{15}N$ values and the marked fields (Fig. 7), following Silva et al. (2012), indicates that the organic matter deposited in the study area is essentially provided by macrophytes, phytoplankton, and algae, as also observed by Alonso-Pérez et al. (2010). According to these authors, the $\delta^{13}C$ values are mainly associated with the algal part in relation to the non-algal portion of the particulate organic carbon. On the contrary, the higher non-algal proportions in particulate organic carbon result in more negative $\delta^{13}C$ values. In core KSGX24, the most negative values of $\delta^{13}C$ are recorded between ≈3000 and 2250 years BP (in the lower section of the core) and could be related to a higher contribution of terrestrial sources of organic matter to the

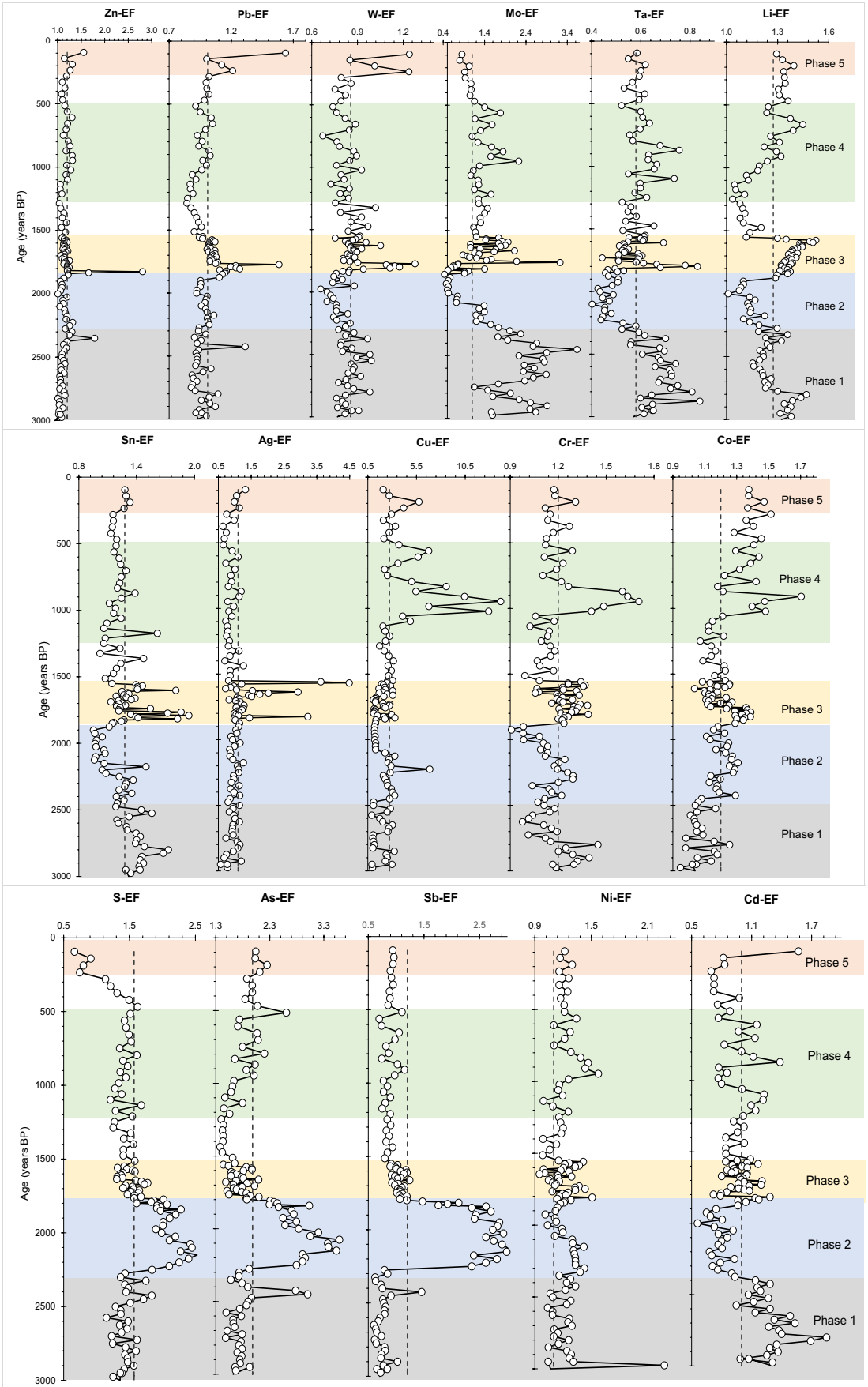
Zn-EF
Pb-EF
W-EF
Mo-EF
Ta-EF
Li-EF
Sn-EF
Ag-EF
Cu-EF
Cr-EF
Co-EF
S-EF
As-EF
Sb-EF
Ni-EF
Cd-EF
Age (years BP)
Phase 5
Phase 4
Phase 3
Phase 2
Phase 1

◂**Fig. 3** Age plots of the enrichment factors (EF) of several chemical element. In the graphs the mean value for each variable is presented (dashed vertical line). Five main phases were identified related to the possible influence of various peoples on mining.

sediments, probably due to a greater fluvial influence in the study area (Schulz and Zabel 2006). The increase in this section of the relative abundance of *Ammonia* spp., which proliferates in disturbed environments under the greater continental influence, also supports this inference (e.g., Bouchet et al. 2021; Debenay and Guillou 2002).

Therefore, factor 2 of the PCA shown in Fig. 6A (Appendix 8) represents the oceanic versus continental influence. The oceanic influence is traced to the increasing values of $\delta^{13}C$ (according to Deines 1980; Lamb et al. 2006; Meyers 1997) and sea urchin, sponges, and bryozoan remains. The continental influence is indicated by the rise of *Ammonia* spp., taxa frequent in coastal transitional waters (Duleba et al. 2018, 2019), with a higher contribution of organic matter from terrestrial productivity and increased concentrations of several lithogenic elements such as Nb, Ti, Ta, Cs, Mo, Zr, and Be.

In addition to higher $\delta^{13}C$ values (Deines 1980; Lamb et al. 2006; Meyers 1997), the increase in MOS and *V. bradyana*, *N. faba*, and *B. spathulata* also suggests higher oceanic influence in the distal sector of Ria de Vigo. The mentioned species are associated with high food supplies and can tolerate oxygen depletion resulting from the consumption and degradation of organic matter by aerobic organisms (Martins et al. 2019). In this area, the increment of oceanic productivity is associated with upwelling events (Prego 1993; Wollast 1998), which should have been stronger on the NW Iberian Margin during several periods in the Late Holocene (e.g., Diz et al. 2002; González Álvarez et al. 2005; Martins et al. 2007, 2013a). The upwelling events typically occur during the spring and summer oceanographic regimes (Álvarez-Salgado et al. 2000; Torres and Barton 2007). Sometimes, however, intense upwelling events occur during the winter (Vitorino et al. 2002) and follow more or less severe rainfall events (Martins et al. 2007) that introduce more freshwater (Pazos et al. 2000; Ríos et al. 1992) into the continental shelf. These phenomena can cause stratification of water masses, with colder, more saline, and denser oceanic water under the low-saline coastal waters (Fraga and Margalef 1979). The stratification in the Ria de Vigo is generally maintained throughout the entire year (Diz et al. 2002). During periods of higher runoff, the rivers transport and introduce more sediments into the Ria de Vigo (Pazos et al. 2000). While the coarser sediments are deposited mainly near the river mouths, the finest ones are transported in suspension and distributed by the currents (Perez-Arlucea et al. 2005). Thus, intense upwelling events occurring under these conditions could eventually produce fronts between the oceanic and coastal waters favorable to the accumulation of fine-grained sediments enriched in trace elements such as Ag, Al, As, Ba, Bi, Co, Cr, Er, Eu, Fe, Ga, Ho, K, Li, Mg, Mo, Ni, P, Pb, S, Sb, Sc, Sr, Tm, U, W, Yb, and Zn (PCA Fig. 6A; Appendix 7) and organic matter, as reported by Martins et al. (2007), for the adjacent continental shelf.

The TOC contents (between 1.50 and 1.95%) in the uppermost 40 cm are markedly high, and the C/S ratio values are relatively low (ranging between 1.6 and 3.8; mean 2.2 ± 0.6; Appendix 1), indicating low oxic conditions, as described by Cetecioğlu et al. (2009). The low oxic condition in the sediments was favorable for the production of sulfides and the formation of siderite and pyrite (Álvarez-Iglesias and Rubio 2008; Rubio et al. 2010) in anoxic and sulfidic environments or microenvironments (Berner 1983; Lin et al. 2020). The presence of these minerals suggests that the supply of organic matter in the study area was high in the last ≈3000 years BP.

Variations in EF-Mn and EF-S values may be largely due to changes in the redox state of the sediment. Under reducing conditions, Mn is depleted (Hastings et al. 2016). The significant enrichment in S (Fig. 3) may instead be related to the production of sulfides in anoxic layers of the sediments (as generically analyzed by Jørgensen et al. 2019). Thus, the variation of the Mn-EF values along the studied core indicates the presence of two redoxcline levels in core KSGX24, the first occurring at ≈2500 years BP and the second at around 500 years BP (Fig. 2), preceding the increase in MOS (Fig. 5) and Fe/Mn values (Fig. 2). The distribution of Fe/Mn values along the core KSGX24 indicates oxygen depletion in the sediments deposited between ≈2300 and 1500 years BP (Fig. 2), which could have been more pronounced around 2000 years BP (Fig. 2). The production of sulfides in this phase may have contributed to the increased values of EF-As, EF-S, and EF-Sb (Fig. 3).

The $\delta^{13}C$ values remained generically higher between ≈2250 and 950 years BP and tended to increase from ≈550 years BP, revealing the presence of a higher proportion of organic matter supplied by oceanic relative to continental sources. These data may have resulted from the strengthening of upwelling events as characterized by Martins et al. (2013a, b) and Piedracoba et al. (2005). However, the increase in MOS between ≈2250 and 1500 years BP and in the last ≈250 years BP suggests that the supply of

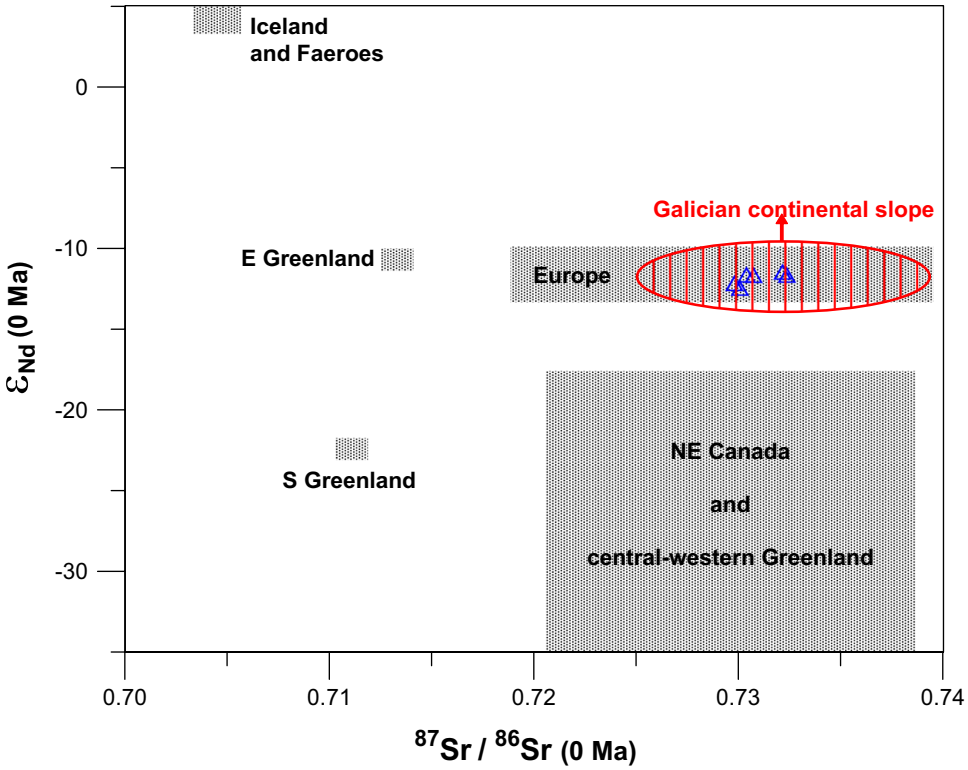

Fig. 4 Sr and Nd isotopic compositions. Blue triangles: terrigenous component of samples from core KSGX 24 (Ria de Vigo). Gray fields: some possible source areas of sediments, with very distinct isotopic compositions, in and around North Atlantic; "Europe" refers, in fact, to western Europe; adapted from Snoeckx et al. (1999), Grousset et al. (2001), and Hemming (2004). Ellipse with red contour: field of compositions of the terrigenous component of sediments from the Galician continental slope, according to the results reported by Martins et al. (2013b) and Plaza Morlote et al. (2017), excluding the samples from layers with ice-rafted debris (clasts with exotic provenance, transported by icebergs in the Pleistocene)

organic matter to the bottom could have been higher during these two periods as well as the stratification of the water masses (traced mainly by the increase of *B. spathulata*). It is also possible that during these two periods, ocean fronts (generated by the clash of coastal and oceanic waters) occurred near the study

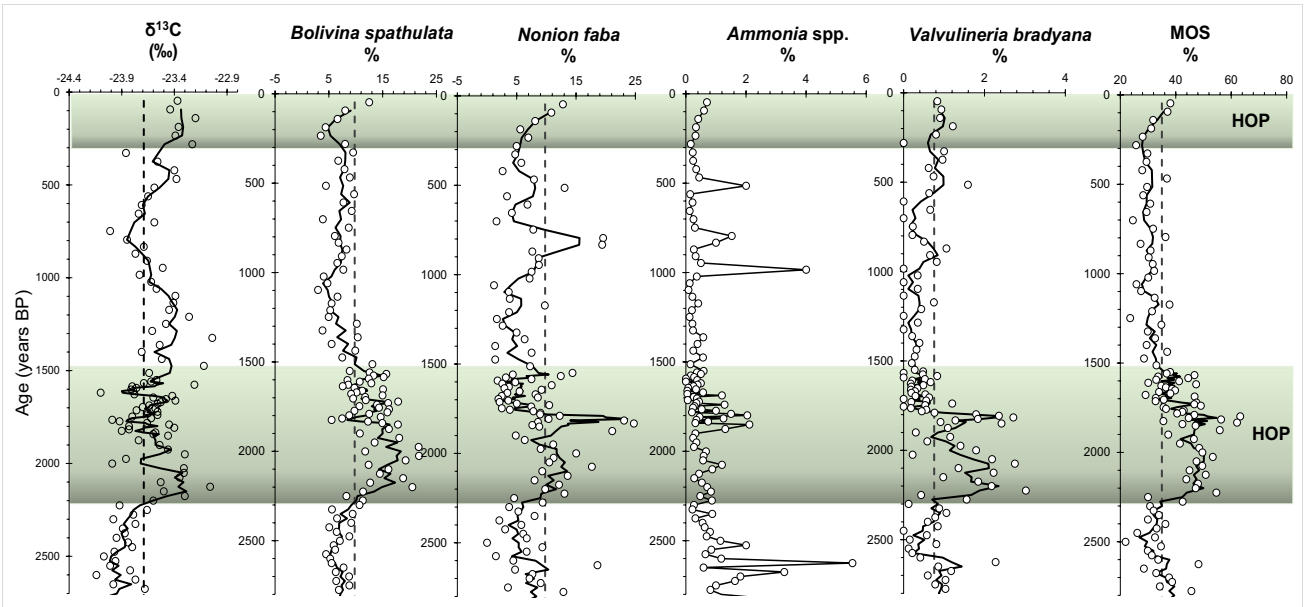

Fig. 5 Values of $\delta^{13}C$, percentage of *Bolivina spathulata*, *Nonion faba*, *Ammonia* spp., *Valvulineria bradyana*, and middle-outer shelf (MOS) species of benthic foraminifera. The mean (dashed vertical line) and the moving average of the values are shown (line between the values (points). Legend: HOP, higher oceanic productivity related to upwelling intensification

area. Identical phenomena were recorded on the adjacent continental shelf by Martins et al. (2007) in both periods.

According to the results of the PCA (in Fig. 6A, B), the finer sediments are negatively correlated to higher foraminiferal abundance and diversity (as indicated by the Shannon index and species richness). Thus, the HOP intervals may have triggered a certain environmental disturbance favoring the development of opportunistic foraminifera. However, the burial of organisms by terrigenous sediments (indicated by the increase in Sc-EF, Ga-EF, Fe/Ca, Mg/Ca, Ti/Ca, and HREE) and the oxygen depletion (suggested by the increase of S-EF, Fe-EF, and Fe/Mn values and a reduction of Mn-EF values; Fig. 2) should have been unfavorable for species with carbonate tests, as suggested by the decline in Ca-EF and Sr-EF (Fig. 2). Calcium and Sr have similar biogeochemical characteristics (Kabata-Pendias and Pendias 1992) and are mostly associated to the biogenic sources of carbonates (e.g., mollusks and foraminifera).

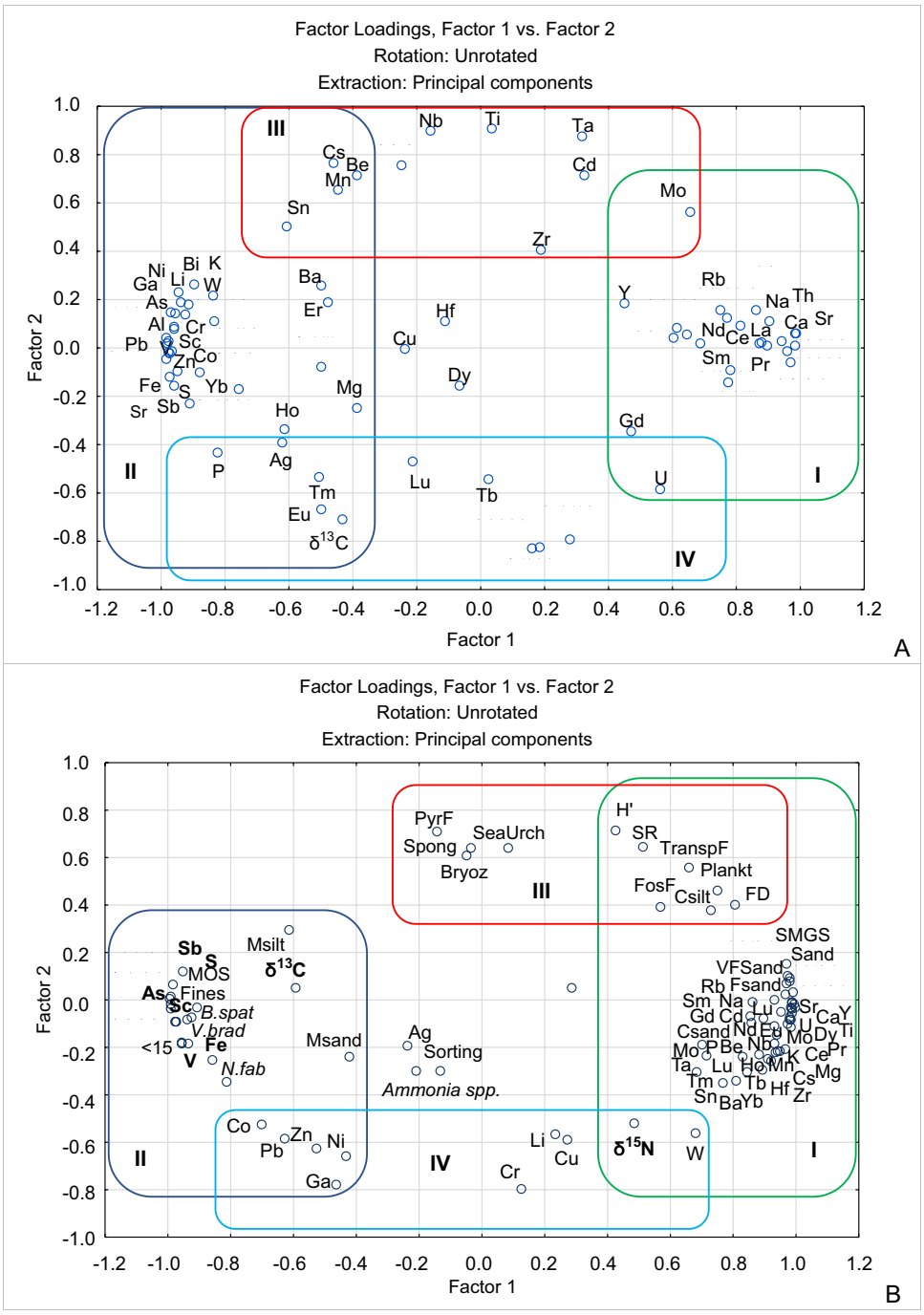

Fig. 6 Biplots of the factor 1 versus factor 2 of two principal component analyses (PCAs) relating elemental concentrations and the enrichment factors (EF) and other geochemical, textural, and biotic variables. Legend: SMGS, sediment mean grain size; VFSand, very fine sand fraction (63–125 μm); Fsand, fine sand fraction (125–250 μm); Csand, coarse sand fraction (> 500 μm); Sand, total sand fractions (> 63 μm); Fines, total fine fraction (< 63 μm); < 15, fine silt and clay fractions (< 15 μm); Msilt, medium silt (15–30 μm); Csilt, coarse silt fraction (30–63 μm). The concentrations of heavy rare earth elements (HREE), $\delta^{13}C$ and $\delta^{15}N$ in organic matter, and several elemental ratios (Th/Sc, La/Sc, Mg/Ca, Fe/Ca, Th/Co, Ti/Ca) were also considered, as well as data related to foraminifera, such as: FD, foraminifera density; SR, species richness; *H'*, Shannon Index; MOS, species more frequent in the middle to outer shelf; N.fab, *Nonium faba*; V.brad, *Valvulineria bradyana*; B.spat, *Bolivina spathulata* and *Ammonia spp*. The abundance of biotic particles found in the sediment also were considered, such as: TranspF, transported foraminifera; Plankt, planktonic foraminifera; PyrF, pyritized foraminifera; Fos, fossil of foraminifera (old tests); SeaUrch, sea urchin spines; Spong, sponge spicules and; Bryoz, bryozoan fragments

On the contrary, FD and SR tended to increase in sandy and coarser-grained sediments (Fig. 6A, B), which are in general associated with more oxic conditions in the sediment, traced by higher values of Mn-EF (Fig. 2; PCA in Fig. 6B). Note that the finer sections are also associated with the enrichment of several potentially toxic elements (PTEs), such as, Co, Ni, Pb, Sb, and Zn, which may have had a negative impact on the benthic fauna.

Detrital sources of sediments

The La/Th vs. Hf discrimination biplot (Fig. 8A) is based on the diagrams of Floyd and Leveridge (1987), Cullers and Podkovyrov (2000), and Bijan Noori et al. (2016), and the ternary Zr-Th-Sc diagram (Fig. 8B), which is based on Bhatia and Crook (1986) and Okunlola and Idowu (2012). The biplot indicates that sediments deposited in the distal region of Ria de Vigo were supplied by rocks formed in a passive margin. This finding perfectly matches with the geological history of the region related to the opening of the northern Atlantic Ocean (Hallam 1971). The biplot of Th/Sc vs. Zr/Sc (Fig. 8C), based on Chen and Robertson (2020), shows that the sediments are related to rocks from the upper continental crust (UCC). The combination of low Cr/V and Y/Ni ratios (both < 1.5) suggests that the main source of the sediments is felsic rocks (Hossain et al. 2017). In addition, the ternary La-Th-Sc diagram (Fig. 8D), based on Cullers and Podkovyrov (2000), indicates that the sediments were mostly sourced by granodiorites, which are present in the Malpica-Tui unit (Gil-lbarguchi 1994; Santos Zalduegui et al. 1995, 1996) and granites, which are abundant in the region (Fuertes-Fuente and Martin-Izard 1994; Llera et al. 2019).

Although hydrographic basins in western Galicia are relatively small and some exotic geological units are present in the region, the Sr and Nd isotopic signature of the terrigenous component of sediments from core KSGX24 fits perfectly into what is expected in materials representative of the western European crust. This part of the continental crust is characterized by having been strongly affected by Paleozoic orogenies (Caledonian and Variscan); therefore, its Sr–Nd isotopic fingerprint is clearly distinct from other possible sources of sediments into the North Atlantic. In the analyzed samples plotted (Fig. 4) within the field of western Europe, although there are mafic and ultramafic rocks in the region and the hydrographic basin is not large, the Sr and Nd isotopic ratios in the sediments were mostly linked with granitoids and metasediments. A hypothetical strong local influence of mafic and ultramafic lithologies on the isotope compositions would have decreased the $^{87}Sr/^{86}Sr$ ratios and increased the ε_{Nd} values relative to typical European upper crustal compositions, but these effects were not observed.

The Malpica-Tui unit (Gil-Ibarguchi and Ortega 1985) and the Galiñeiro Complex (Montero et al. 1998), which cross the Ria de Vigo, have abundant bastnasite, parisite, xenotime, thalenite, and yttrialite (Marmolejo-Rodríguez et al. 2008). Yttrium is a trace element in the Earth's crust (mean 33 mg kg^{-1}; Taylor 1964) but is concentrated in some minerals, especially xenotime and monazite (Montero et al. 1998), which are present as accessory phases in granitic gneiss, igneous, and metamorphic rocks that occur around the Ria de Vigo (Evans et al. 2003; Nombela et al. 1995). These minerals are resistant to chemical weathering and tend to be preserved in the detrital component of the sediments. Yttrium is also considered to have little involvement in

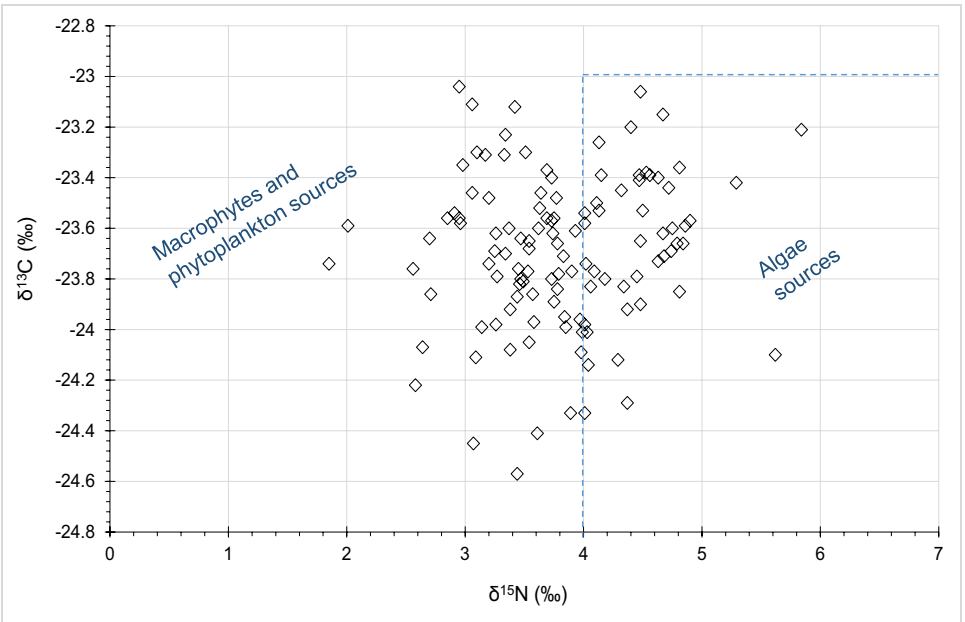

Fig. 7 Values of $\delta^{13}C$ vs. $\delta^{15}N$. The fields were marked according to Silva et al. (2012)

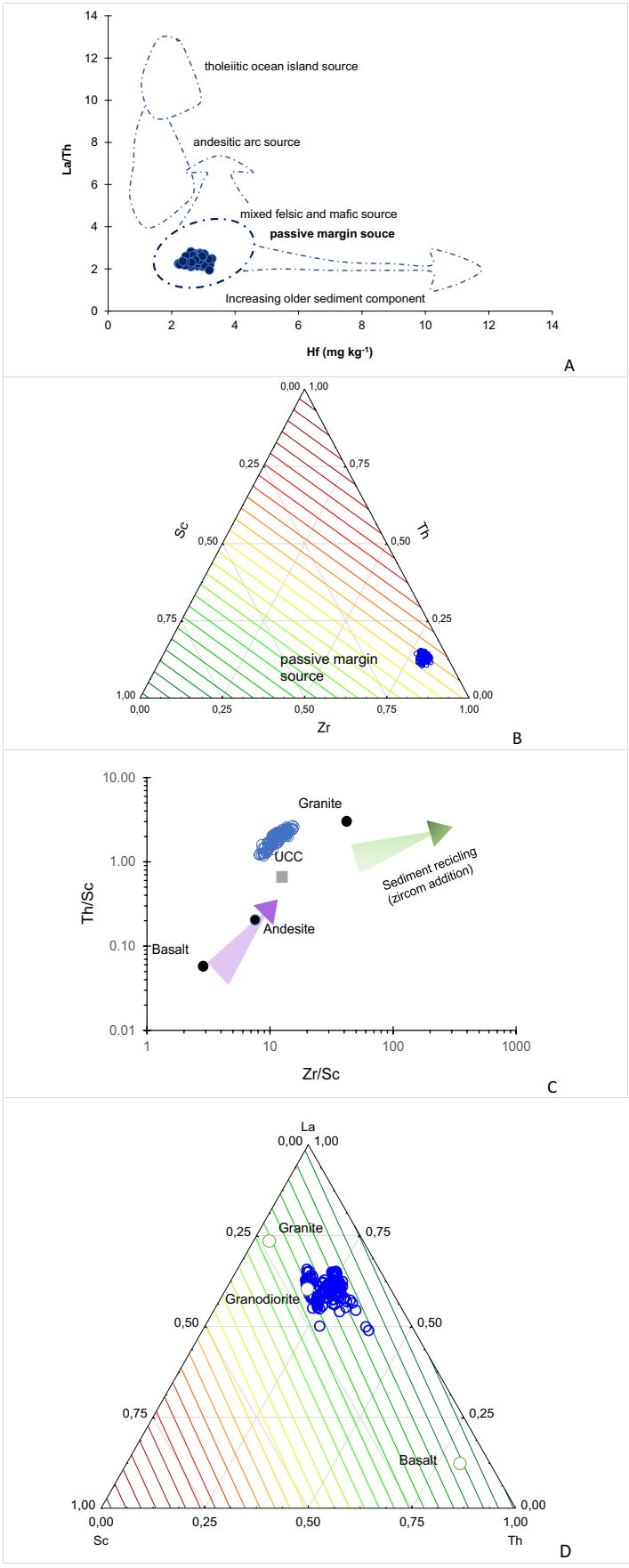

Fig. 8 **A** Source rock La/Th vs. Hf discrimination diagram (based on the diagrams of Floyd and Leveridge 1987; Cullers and Podkovyrov 2000; Bijan Noori et al. 2016). **B** Ternary Zr–Th–Sc diagram (based on Bhatia and Crook 1986 and Okunlola and Idowu 2012). **C** Biplot of Th/Sc vs. Zr/Sc (based on Chen and Robertson 2020). **D** Ternary La–Th–Sc diagram (based on Cullers and Podkovyrov 2000). Legend: UCC, upper continental crust

diagenetic processes. Therefore, it has been used to relate the sediments to the source rocks (Murad 1978), and the concentrations of this element provide insights into the weathering of the rocks surrounding the Ria de Vigo and the transport of sediments from this coastal system toward the adjacent continental shelf (Marmolejo-Rodríguez et al. 2008).

Yttrium concentrations (between 10.4 and 13.1 mg kg^{-1}; mean 11.5 ± 0.5 mg kg^{-1}) along the core KSGX24 can be considered pristine (EF values < 1). This element is more enriched in coarser intervals (PCA in Fig. 6B). This would be expected since, according to Turekian and Wedepohl (1961), the worldwide sands have higher mean concentrations of Y (40 mg kg^{-1}) than shale (26 mg kg^{-1}). In surface sediments of the Ria de Vigo, the enrichment of this element is mostly observed in its middle zone and is also related to sands (Marmolejo-Rodríguez et al. 2008). The PCA results (Fig. 6 (II)) and the correlations presented in Appendix 7 show that Y-EF is associated with the enrichment of several other chemical elements (La-EF, Ce-EF, Pr-EF, Th-EF, Y-EF, Rb-EF, Nd-EF, Sm-EF, Zr-EF, Na-EF, Ti-EF, Gd-EF, K-EF, Hf-EF, Mg-EF, Ta-EF, U-EF, Tb-EF, Dy-EF, Nb-EF, Er-EF, Lu-EF, Cs-EF, Yb-EF, Cd-EF, Eu-EF, Mo-EF, Ho-EF, Be-EF, Ba-EF, Sn-EF, P-EF, Mn-EF, W-EF), as well as the ratios La/Sc, Th/Sc, and Th/Co. Therefore, the ratios Ti/Ca, Fe/Ca, and Mg/Ca can be considered good tracers of the lithogenic influx relative to the biogenic influx (Gebregiorgis et al. 2020; Nace et al. 2014).

Since Th/Co is not affected by biogeochemical processes that occur in bottom sediment (Taylor and Mclennan 1985), it is also used as an important proxy for determining the source area of the sediments and the chemical composition of the rocks (Cullers and Podkovyrov 2000). Similarly, the Th/Sc (Condie 1993; McLennan et al. 1993) and La/Sc (Cullers 2002) ratios along the core KSGX24 also indicate that a sedimentary contribution essentially originated from felsic rocks, possibly derived from the Variscan granitoids that make up the Galicia-Trás-os-Montes Zone (Dias da Silva et al. 2016). These ratios reach their highest values in the coarser intervals and decrease in the finer ones, in opposition to the rise of HREE, Ti/Ca, Fe/Ca, and Mg/Ca (Figs. 3 and 6B).

Although the sediments of the analyzed core are generally depleted in relation to HREEs (average, 24.1 mg kg^{-1}), their concentrations slightly increase in the finest layers, reaching 29.2 mg kg^{-1} (Fig. 2). The finer-grained intervals are also characterized by higher proportions of phyllosilicates, chlorite, and siderite, as described by Martins et al. (2016), which also indicates a higher contribution of detrital particles (Fig. 6B). Thus, the finer-grained intervals could have been characterized by a reduction in the contribution resulting from felsic rocks (Fig. 3) and a higher supply of materials from mafic and ultramafic complexes that underlie much of the region (Farias et al. 2014; Fig. 1D). These variations may also be influenced by changing patterns of rock weathering and sediment supply, which may be related to changes in climatic or oceanographic processes (as analyzed by Diz et al. 2002; González Álvarez et al. 2005; Martins et al. 2007, 2013a).

Sources of paleopollution

Taking the Sutherland (2000) classification as a reference, some sedimentary layers of the KSGX24 core can be considered significantly enriched in Cu-EF and moderately enriched in Ag-EF, Mo-EF, As-EF, Sb-EF, S-EF, Zn-EF, Ni-EF, Sn-EF, Cd-EF, Cr-EF, Co-EF, Pb-EF, and Li-EF (Appendix 1). Whereas the increase of Mo-EF, Sn-EF, and Cd-EF is essentially associated with coarser sediments (and sandy fraction content; Fig. 6B; Appendix 7), Li-EF is positively correlated with medium silt and medium sand fractions. Meanwhile, Cr-EF is negatively correlated with coarse silt fractions but is weakly correlated to the other fractions. Ag-EF has a low correlation with grain size, and As-EF, S-EF, Sb-EF, Zn-EF, Ni-EF, Co-EF, and Pb-EF are found in finer-grained sediments, as mentioned.

According to the classification and terminology of Müller (1986) for Igeo values (Appendix 1; Fig. S1), we can infer that the core KSGX24 has sediment layers moderately to strongly polluted by Cu and As and moderately polluted, for instance, by Ag, Sb, Mo, S, Zn, and Ni, as well as by Sn, Pb, Cd, V, Co, Cr, Fe, and W (Appendix 1). Based on EF and Igeo values, several instances of pollution can be identified in core KSGX24 (Figs. 2, 3, and 9), as described below.

Phase 1, ≈3000–2750 years BP

Phase 1, ≈3000–2750 years BP, with a moderate increase of Cd, Ni, Sn, and Cr, is characterized by low $\delta^{13}C$ and MOS values and a relatively high content of lithogenic chemical elements and peaks of *Ammonia* spp., which indicates higher continental influence, a higher supply of organic matter from continental sources, and relatively low oceanic productivity. The relatively high Th/Co, Th/Sc, and La/Sc values indicate that the materials supplied were felsic rock granitoids and high-grade gneisses and mica-schists with a similar major element composition to granite (Evans et al. 2003; Llera et al. 2019; Nombela et al. 1995).

It is known that the inhabitants of Galicia advanced in the use of the minerals from classical times (Comendador Rey et al. 2016; Meunier 2011). This phase of metal enrichment was noticed by Martínez-Cortizas et al. (1997a) in the

Penido Vello bog (NW Spain) by the slight rise of Pb and Cd, which was attributed to atmospheric pollution caused by Late Bronze Age mining activities.

In the core KSGX24, the general enrichment of, for instance, Cd, Ni, Sn, and Cr (and Ag, As, Co Cr, Pb, Sb, Sn, and Zn, but also Al, Be, Bi, Cs, Eu, Fe, Ga, Ho, Mn, Sc, S, and Tm; Appendix 7; Fig. 6A), is associated with increasing Li and a rise in Ta in some layers (Figs. 2 and 3), probably due to mining, as observed in other regions of the world (Muhly 1973, 1988; Weeks 2003). Mineralizations with these elements occur in quartz veins containing sulfides (mainly pyrite, arsenopyrite, and chalcopyrite) and are associated with hydrothermal processes in fractured host granites (Urbano et al. 1998). In Central Galicia, there are both barren and Li–Sn–Ta–mineralized pegmatites. In both bodies, the pegmatite-derived fluids that migrated into the wall rock are enriched in several elements, such as Li, Rb, Cs, Sn, Zn, and As (Llera et al. 2019).

It is possible that mining activity occurred in areas drained by rivers that discharge into the Ria de Vigo and drain areas with a number of spodumene-bearing pegmatites, some quite extensive (Parga-Pondal and Cardoso 1948). These pegmatites have several accessory minerals, including beryl ($Be_3Al_2Si_6O_{18}$), columbite-tantalite [columbite: (Fe, Mn) Nb_2O_6; Ta atoms can replace niobium atoms in the columbite structure and form tantalite), apatite [$Ca_5(PO_4)_3(F,Cl,OH)$], some heterosite [$(Fe^{3+},Mn^{3+})PO_4$], and ferrisicklerite [$Li_{1-x}(Fe^{3+}{}_xFe^{2+}{}_{1-x})PO_4$] derived from lithiophilite triphylite (a series from $LiMn^{2+}PO_4$ to $LiFe^{2+}PO_4$), zircon ($ZrSiO_4$), arsenopyrite (FeAsS), and manganiferous garnet, mainly in the contact zones (Von Knorring and Vidal Romani 1981). According to these authors, columbite-tantalite is embedded in cleavelandite [$(Na(AlSi_3O_8)$] and dispersed in a fine-grained albite-rich matrix ($NaAlSi_3O_8$) of the main pegmatite. Tantalite [(Fe, Mn)(Ta, Nb)$2O_6$] has some inclusions of a tin-bearing phase similar to the mineral wodginite ($Mn_2+Sn_4+Ta_2O_8$), and garnets and phosphates in Li-pegmatites are frequently rich in manganese. Thus, the chemical elements whose enrichment is associated with the positive axis of factor 1 of the PCA in Fig. 6B (I) could be mostly associated with this type of contribution in the study area.

Nickel often occurs associated with copper deposits and is present in continental soils. The distribution pattern of Cd along the core KSGX24 is similar to that of Be, Cs, Hf, Nb, Rb, Th, and Ti (as indicated by the positive and significant correlations with these chemical elements; Appendix 7), and is associated to Ta increases, suggesting common lithogenic sources. The Li–Sn–Ta–mineralized pegmatites are also associated with sulfides, such as sphalerite (ZnS), the primary ore of Cd, occurring as an impurity. The sphalerite formation was probably related to a post-magmatic hydrothermal event (Llera et al. 2019). However, according to Nriagu (1979), an important natural source of Cd is volcanic emissions. It is possible that atmospherically transported materials also contributed to the increase of Cd, as there was a considerable increase in northern European volcanic ash (NEVA) during this period (Swindles et al. 2018). Note that during the Holocene, there were, for example, more than 20 eruptions per century in Iceland from about 30 active volcanoes (Thordarson and Höskuldsson 2008). The recent eruption in 2010 of the Eyjafjallajökull volcano (Iceland), linked with particular meteorological conditions, resulted in the dispersal of volcanic ash over large areas of the North Atlantic Ocean and Europe (e.g., Gasteiger et al. 2011; Gudmundsson et al. 2012). Volcanic activity events also occurred in the Azores (Andrade et al. 2021; Moore 1990) during the periods when the highest Cd peaks were recorded in the KSGX24 core, which also supports the hypothesis of fluxes deriving from atmospheric deposition (agreeing with the observations in peat cores of López-Merino et al. 2014; Martinez Cortizas et al. 2005, 2012, 2013, 2016; Olid et al. 2010, 2013; Pontevedra-Pombal et al. 2013).

Phase 2 (≈2450–1850 years BP)

Phase 2, ≈2450–1850 years BP, with a sharp increase of As-EF, S-EF, and Sb-EF, and peaks of other elements (Co-EF, Cr-EF, Cu-EF, Ni-EF, Pb-EF, Sn-EF, and Zn-EF), is characterized by a rise of $\delta^{13}C$ and MOS. The occurrence of As-enrichment in "As-rich pyrite," which also contained, for example, Sb, Ni, Pb, Co, Cu, and Zn and related geological settings, was indicated by several authors (e.g., Cepedal et al. 2008; Jahoda et al. 1989; Gutiérrez Claverol et al. 1991; Piering et al. 2000), mainly in NW Galicia. Thus, it is possible that in addition to materials transported by the rivers, contributions were also received from the atmosphere. This phase has also been described, for example, by Martínez-Cortizas et al. (1997a) and Pontevedra-Pombal et al. (2013) in peat cores from the NW Iberia, where increased concentrations of As, Cd, Ni, Pb, and Zn were observed. These and other authors have assigned this contamination to mining during the Iron Age (López-Merino et al. 2014; Martinez Cortizas et al. 2005, 2012, 2013, 2016; Pontevedra-Pombal et al. 2013).

The geochemical, granulometric, and faunal characteristics suggest that upwelling events were more intense during this period, giving rise to stronger stratification of the water column. Additionally, oceanic fronts might have occurred near the study area that favored the deposition of finer sediments and a greater expression of materials from mafic and ultramafic complexes (as suggested by the decreasing of Th/Co, Th/La, and La/Sc; Fig. 2) that outcrop in the region (Fig. 1D). Oceanic productivity was also higher, as seen in the flux of organic matter to the bottom, which should have given rise to a greater scarcity of oxygen and higher diagenetic processes (García-García et al. 1999), indicated by the rise of V-EF and Fe/Mn.

Phase 3 (≈1850–1550 years BP)—Roman mining

Phase 3, ≈1850–1550 years BP, showed peaks of Ag-EF, Co-EF, Cr-EF, Pb-EF, Sn-EF, W-EF, and Zn-EF, associated with a marked increase in Li-EF and Ta-EF. The peaks of these elements were probably related to intense mining activity that developed during the Roman times, when many new mines were established in the region (Martínez-Cortizas et al. 2002; Roos-Barraclough et al. 2002; Rosman et al. 1997). Silver was a product extracted from the region, which had a greater profitability than gold given the technical possibilities existing at the time (Pérez-García et al. 2000; Hillman et al. 2017). Moreover, copper, tin, iron, and lead were extracted (O'Brien 2015), as well as sulfur (Figueiredo et al. 2018).

Metallurgy on the Iberian Peninsula contributed almost 40% of the world's Pb production during the Roman Empire (Nriagu 1983). Note that this activity has also been recorded in Greenland, with peak concentrations of lead and copper (Hong et al. 1994, 1996). The Pb increase in this period agrees with the record of a prominent increase of lead in peat cores from NW Spain related to the exploitation of alloys (Killick and Fenn 2012; Kylander et al. 2005; López-Merino et al. 2014; Martínez-Cortizas et al. 1997a, 2002, 2005, 2012, 2013, 2016, 2020; Pontevedra-Pombal et al. 2013). Thus, part of the Pb increases observed in core KSGX24 could be related to atmospheric Pb pollution (which began at least ≈2800 years ago due to Pb mining and metallurgy in Spain), air transport from Saharan aridification, and a large expansion of agricultural practices in NW Spain (Kylander et al. 2005; Martínez Cortizas et al., 1997b).

Arsenic and tin were also exploited in the same districts as gold pyrite (Arias et al. 2008), which has been mined in different periods from the Bronze Age to modern times (Comendador Rey et al. 2016), but mostly during Roman times (Duarte 1995). These elements are related to diverse types of hydrothermal deposits, which are more abundant infilling microfractures functioning as conduits for hydrothermal fluids in arsenopyrite or included in pyrite and frequently associated with galena (e.g., Cepedal et al. 2013; Martínez-Abad et al. 2015).

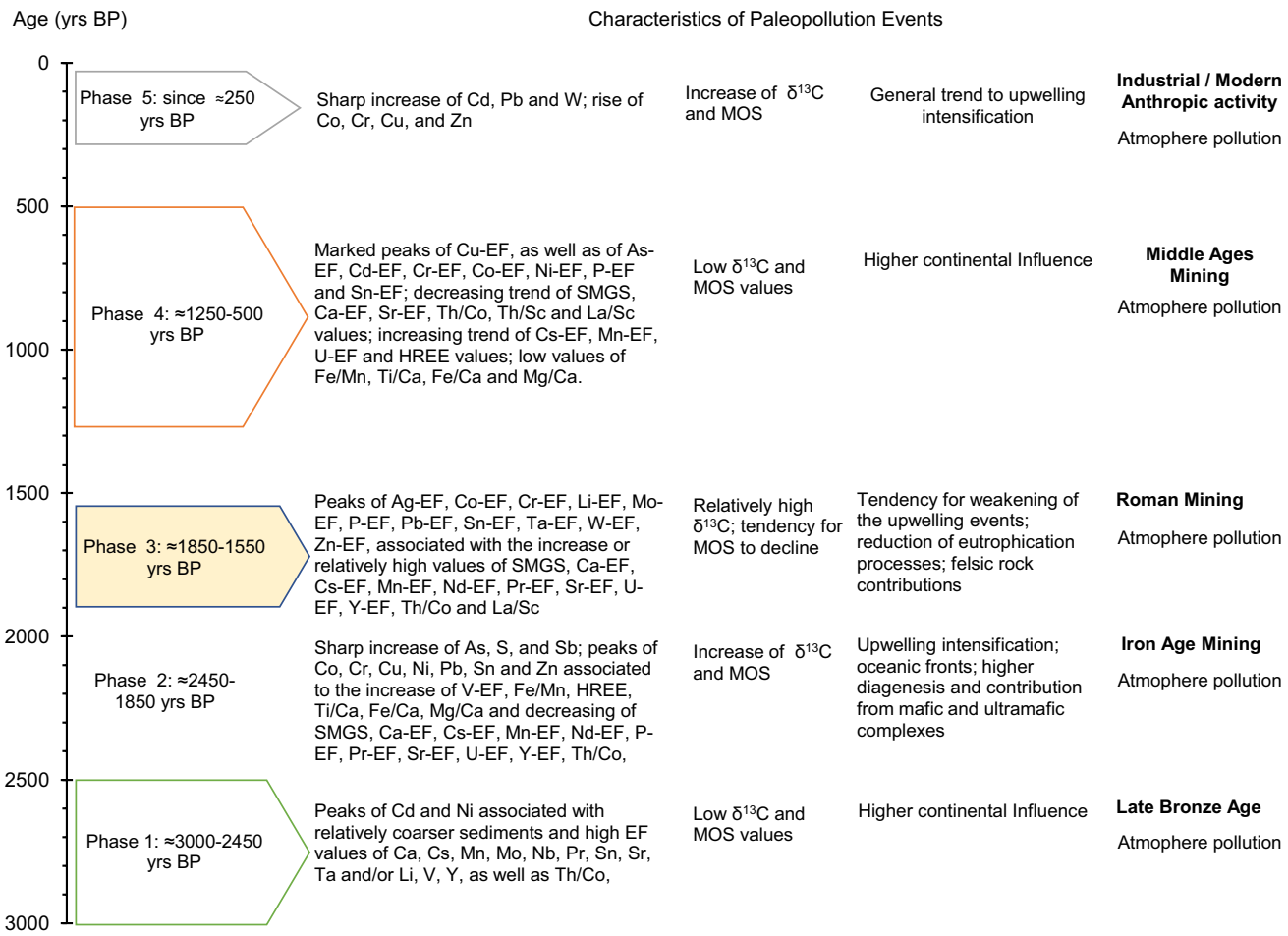

Fig. 9 Schematic overview of the characteristics of paleopollution events

Zinc followed a similar pattern to Pb in the core KSGX24 (Fig. 3) but with sharper peaks during Roman times. The source of Zn may have been the same as that of Pb since in NW Spain mining took place mainly in Hercynian granitoids in the form of vein and stratiform deposits in siliciclastic and calcareous rocks containing Zn–Pb (Tornos et al. 1996; Velasco et al. 1996).

Therefore, sediments resulting from mining activity during Roman times may have been transported by rivers to the Ria de Vigo but were probably also dispersed through the atmosphere, as observed in peat bogs from NW Iberia by Martínez-Cortizas et al. 1997a, 2005, 2012, 2013, 2016), Pontevedra-Pombal et al. (2013), and López-Merino et al. (2014).

The Roman mining period (≈1850–1550 years BP) was also characterized by relatively high $\delta^{13}C$ and *Ammonia* spp. values and by a tendency for MOS to decline (Fig. 5). In addition, the period saw relatively high values of Th/Co and La/Sc and a tendency for increased values of SMGS, Ca-EF, Sr-EF, and Mn-EF, which together can be interpreted as a tendency for a weakening of upwelling events, reduction of eutrophication processes, augmentation of carbonated biogenic particles, and a dilution of contributions from mafic and ultramafic rocks (Fig. 9).

Phase 4 (≈950–500 years BP)—Late Antiquity and Middle Ages mining

Phase 4, ≈950–500 years BP, is characterized by the occurrence of a sharp increase in Cu, associated with peaks of As, Cd, Cr, Co, and Ni, and a rise in Ta-EF and Li-EF values. This period is related to mining activities in the Late Antiquity and Middle Ages. The main raw materials from which Cu is extracted include pyrrhotine and chalcopyrite in granatiferous amphibolites, which are considered to be of volcanosedimentary origin (Arias et al. 2008) and also enriched in Cr and Co. This phase also demonstrated a slight rise of Pb in the Penido Vello bog (NW Spain), as shown in Martínez Cortizas et al. (1997b).

The increase of these metals occurred in a phase in which there is a decreasing trend of SMGS, Ca-EF, Sr-EF, Th/Co, Th/Sc, and La/Sc values; an increasing trend of Cs-EF, Mn-EF, U-EF, and HREE values; and low values of Fe/Mn, Ti/Ca, Fe/Ca, Mg/Ca, $\delta^{13}C$, and MOS. Taken together, these data indicate a higher continental influence, lower flux of organic matter to the bottom, and more aerated conditions in the sediment, but tend toward a new period of increasing influence of upwelling events in the Ria de Vigo.

Phase 5 (from ≈250 years BP)—industrial and modern anthropic activities

Phase 5, from ≈250 years BP, is characterized by a sharp increase in Cd, Pb, and W and a rise in Co, Cr, Cu, and Zn, associated with relatively high Li-EF values. This event is related to industrial and modern anthropic activities and has also been described by several authors (e.g., Kylander et al. 2005; Olid et al. 2010; Pontevedra-Pombal et al. 2013). On the one hand, significant peaks of Cu in peat cores have also been observed in the last 250 years BP, mainly resulting from local pollutant sources (i.e., coal mining and burning) under the influence of regional and local atmospheric metal deposition (Martínez Cortizas et al. 1997; Olid et al. 2010; Pontevedra-Pombal et al. 2013). On the other hand, Cd is a quite mobile element—its enrichment can be related to bacteria-mediated processes of solid sulfide mineral production (Davies-Colley et al. 1985) or with the formation of organic-Cd complexes (Macías and Calvo de Anta 2008).

In Galicia, during the first half of the twentieth century, the production of tin and tungsten had a few years of expansion closely linked to armed conflicts, mainly to the Second World War (WWII; Rodríguez Pérez 1985; Comendador Rey et al. 2016). During WWII, the need for wolfram (W) arose from the Allies (England) and Nazi Germany, establishing a conflict of interest in the NW zone of the Iberian Peninsula that is known as the "war of the wolfram" (Lage 2020), which was largely controlled by the Germans (Lage 2020; Wheeler 1986). Extensive atmospheric deposition of lead has been caused by a variety of factors (Renberg et al., 2001), including the Industrial Revolution, mining activity, adding lead to gasoline in recent times, fly ash from incinerators, coal combustion, wastewater outflows, harbor-shipyard activities, and the use of fertilizers and pesticides in agriculture (Ramírez-Pérez et al. 2020). This Pb increase has also been detected in peat cores (Olid et al. 2010, 2013; Martínez Cortizas et al. 2012).

This phase is associated with an increase of V-EF, $\delta^{13}C$, and MOS values; a decrease of SMGS, Ca-EF, Mn-EF, Sr-EF, Th/Co, Th/Sc, and La/Sc; and a trend to increasing Fe/Mn values. Taken together, these data indicate a higher marine influence, a higher flux of organic matter supplied by oceanic productivity to the bottom, a trend to oxygen depletion in the sediment, and a general trend to upwelling intensification (Fig. 9).

Final considerations

Regarding paleoclimatic and paleoceanographic conditions, two main phases of intensification of upwelling events have been identified (Fig. 9). The upwelling events favor the deposition of muddy sediments rich in organic matter, culminating in a stratified shelf and a weak benthic hydrodynamic regime (Jouanneau et al. 2002; Martins et al. 2007), which agrees with the results described in core KSGX24. Considering atmospheric circulation, these changes should be an indicator of the interference of the North Atlantic Oscillation (NAO), a large-scale atmospheric circulation mode in the region (Giradeau et al. 2000; Hurrell 1995; Hurrell et al. 2001), as well as the occurrence of cycles of solar activity (Bond et al., 2001), which lead to variations in ocean current intensity (Bianchi and McCave 1999). Note that the

intensification of precipitation and high sea surface temperatures (SSTs) in the Iberian Peninsula is correlated with a negative NAO index (Hurrell 1995; Ribeiro et al. 2016), while the intensification of the north wind, which drives the coastal upwelling along the W Iberian Margin, is correlated with positive NAO indices (Abrantes et al. 2005).

The mobilization of materials resulting from mining operations (Bury 2005; Duarte 1995; Lima 2011) might have been a source of sediments in the study area. The mobilization of lithogenic materials could also have been facilitated by the dynamics of deforestation and agricultural intensification (Carrión et al. 2010; Kaal et al. 2011; López-Merino et al. 2012, 2014; Martínez Cortizas et al., 2006, 2020; Mighall et al. 2006; Sanchez Pardo 2013; Silva-Sánchez et al. 2014). Vegetation underwent major changes during the Bronze and Iron Ages, the Roman period, and with the permanent decline of deciduous forests since the Middle Ages as agriculture and metallurgy intensified (Mighall et al. 2006).

Note that the paleopollution records related to paleomining activities described in core KSGX24 (composed of marine sediments; Fig. 9) are also recorded in other transitional systems (e.g., Irabien et al. 2012, 2020) and in peat bogs from N Spain (Kylander et al. 2005; López-Merino et al. 2014; Martínez-Cortizas et al. 1997a, 2005, 2012, 2013, 2016; Olid et al. 2010, 2013; Pontevedra-Pombal et al. 2013), as mentioned above. The work performed in peat cores revealed that the paleopollution recorded in bogs resulted from pollution through the atmosphere with isotopic signatures similar to lithologies present in Northern Iberia. Therefore, it is also possible to assume that airborne materials, notably from mining regions at the N, NE, and E of the Ria de Vigo, may have contributed to the levels of paleopollution recorded in core KSGX24. Most paleopollution events recorded in core KSGX24 are associated with increased Li and/or Ta, suggesting common sources of the contaminants from mineralized pegmatites occurring in the region (Canosa et al. 2012; Fuertes-Fuente and Martin-Izard 1994; Fuertes-Fuente et al. 2000; Llera et al. 2019). However, an exception to this general trend was observed in phase 2, ≈2450–1850 years BP, in which a significant reduction of Li and Ta contents was recorded in core KSGX24 (Fig. 3). This event was characterized by a sharp increase of As, S, and Sb and peaks of several metals (e.g., Co, Cr, Cu, Ni, Pb, Sn, and Zn; Fig. 3). Moreover, the event appears to have been recorded during a period of upwelling intensification, which gave rise to the development of oceanic fronts in the distal sector of Ria de Vigo, generating a high degree of eutrophication and intense diagenesis processes (Fig. 9). The intensification of upwelling processes in the distal region of the Ria de Vigo seems to favor the accumulation of minerals from mafic and ultramafic complexes, while it is probable that the lithic components richer in felsic components are mainly accumulated in more internal areas of this system.

Licht and Plawiak (2005) observed that oxidizing conditions tend to promote Fe precipitation as oxides and hydroxides. However, under reducing conditions linked with a high supply of organic matter to the sedimentary environment, Fe can be sequestered during sulfide mineral formation. Strong indicators that Fe is mainly retained in this sedimentary phase are shown by the presence of pyrite in the sediments and foraminiferal tests along the core KSGX24 (Appendix 7).

The study area's protection by the Cies Islands and the paleoceanographic processes might have facilitated the relatively high accumulation of organic matter and the deposition of fine sediments, which induced diagenetic processes. Several redox-sensitive and sulfide-forming elements, such as Ni, Sb, and Zn, could have been retained in this phase (Álvarez-Iglesias and Rubio 2012, 2020; Yano et al. 2020). These processes were favorable to the maintenance of paleopollution records in the last 3000 years BP in the distal sector of Ria de Vigo, mostly during phases 2 and 5. On the contrary, the more hydrodynamic phases associated with downwelling events gave rise to gaps in the paleopollution record or might result in a more nuanced picture of human influence in the study area. However, the results obtained reveal that the sediments from core KSGX24 are strongly to moderately polluted by Cu between 5 and 45 cm, As between 1 and 39 cm and 130 and 173 cm depth, and show moderate pollution by Pb, Cd, and Co between 0 and 1 cm depth. Although part of the concentrations of these metals may be retained in sulfides, the remobilization and aeration of the sediments can facilitate the reintroduction of the metals into the water column and become a source of risk to the biota.

Conclusion

The grain size, geochemical, and microfaunal records acquired along core KSGX24 were conditioned by natural and anthropogenic factors over the last 3000 years. Although this core consists of muddy sediments whose mineralogical component is essentially supplied by felsic rocks outcropping in the region, finer layers seem to contain a relatively higher output from mafic and ultramafic rocks (which cross the Ria de Vigo). These finer layers follow the strengthening of upwelling phenomena due to the prevalence of positive NAO phases and the intensification of the northerly wind.

The strengthening of upwelling events may have given rise to a greater stratification of water masses and influenced the generation of oceanic fronts near the study area, located in the distal sector of the Ria de Vigo. These fronts favored a greater accumulation of organic matter, which could have given rise to more intense diagenetic processes

leading to the formation of sulfides and facilitating the retention of Fe, S, and other metals sensitive to redox conditions, mainly between ≈2250 and 1500 years BP and in the last ≈250 years BP.

In addition, several layers of polluted sediments were identified in the distal region of the Ria de Vigo associated with different phases of mining related to the Late Bronze Age (≈3000–2450 years BP), Iron Age (≈2450–1850 years BP), Roman times (≈1850–1550 years BP), Middle Ages (≈1250–500 years BP), and industrial and modern (≈250–0 years BP) anthropic activities. The enrichment of metals (such as As, Cu, Ag, Sb, Mo, S, Zn, Ni, Sn, Pb, Cd, V, Co, Cr, Fe, and W) in these periods seems to be related to the mobilization of sediments eroded from the rocks of the region. These materials may have been transported by rivers and even ocean currents and accumulated depending on favorable oceanographic and sedimentary conditions, as mentioned. However, the area also could have received contributions through the atmosphere from the remobilization and transportation of particles from mined areas in E, NW, and NE Iberia and even from volcanic eruptions. However, this hypothesis still needs to be confirmed in future studies by using isotopes (for example, Pb, which allow tracing the source of contamination by this chemical element) and its comparison with data obtained in peat cores. The enrichment in metals in the last ≈250 years BP was also a consequence of industrial and modern anthropic activities.

Mining and anthropogenic activities gave rise to sediments moderately polluted by Pb, Cd, and Co (between 0 and 1 cm depth of the sedimentary column), moderately to strongly polluted by As between 0 and 39 cm and 130 and 173 cm, and Cu between 5 and 45 cm in depth. Some of these pollutants may be trapped in sulfides. However, if the sediments are remobilized and the sulfides are degraded by oxidative processes, the metals may reenter the water column and affect the biota.

Supplementary Information The online version contains supplementary material available at https://doi.org/10.1007/s11356-022-20607-1.

Acknowledgements The authors would like to thank the editor, the anonymous reviewers, and Professor Antonio Martínez Cortizas for their collaboration in the improvement of this work. The authors would like to thank Professors Jean Marie Jouanneau and Olivier Weber from Université Bordeaux I for the material transfer. Funds for Dr. Martínez-Colón were provided by the Sloan Scholars Mentoring Network (SSMN) from the Social Science Research Council.

Author contribution All authors approved the manuscript. Maria Virginia Alves Martins: conceptualization, methodology, data acquisition, data curation, and investigation, writing—original draft. Lucas Cazelli: writing—original draft. Missilene Yhasnara: writing—original draft. Layla Cristine da Silva: writing—original draft. Murilo Barros Saibro: writing—original draft. Fabia Emanuela Rafaloski Bobco: writing—original draft. Belen Rubio: writing—original draft. Bruna Ferreira: data acquisition. Wellen Fernanda Louzada Castelo: writing—original draft. José Francisco Santos: writing—original draft. Sara Ribeiro: data acquisition. Fabrizio Frontalini: writing: original draft. Michael Martínez-Colón: writing—original draft. Egberto Pereira: writing: original draft. Luzia Antonioli: writing—original draft. Mauro Geraldes: writing: original draft. Fernando Rocha: funding acquisition and resources. Silvia Helena Mello e Sousa: Investigation. João Manuel Alveirinho Dias: funding acquisition, project administration, and supervision.

Funding The authors would like to thank the Conselho Nacional de Desenvolvimento Científico e Tecnológico of Brazil, CNPq (project processes #443662/2018–5 and #302676/2019–8 to MVAM), Fundação Carlos Chagas Filho de Amparo à Pesquisa do Estado do Rio de Janeiro, FAPERJ (project processes: E-26/202.927/2019 to MVAM) Brazil, and Fundação para a Ciência e a Tecnologia (FCT, Portugal; the strategic project UID/GEO/04035/2019) for financial support.

Data availability All data were made available as supplementary materials.

Declarations

Ethics approval The authors followed the ethical standards.

Consent to participate The authors have consent to participate.

Consent to publish The authors have consent from institutions to publish.

Competing interests The authors declare no competing interests.

References

Abrantes F, Lebreiro S, Rodrigues T, Gil I, Bartels-Jonsdottir H, Oliveira P, Kissel C, Grimalt JO (2005) Shallow-marine sediment cores record climate variability and earthquake activity off Lisbon Portugal for the last 2000 years. Quatern Sci Rev 24:2477–2494

Alonso-Pérez F, Ysebaert T, Castro CG (2010) Effects of suspended mussel culture on benthic–pelagic coupling in a coastal upwelling system Ria de Vigo, NW Iberian Peninsula. J Exp Mar Biol Ecol 3822:96–107. https://doi.org/10.1016/j.jembe.2009.11.008

Álvarez-Fernandez N, Martínez Cortizas A, López-Costas O (2020) Atmospheric mercury pollution deciphered through archaeological bones. J Archaeol Sci 119:105159. https://doi.org/10.1016/j.jas.2020.105159

Álvarez-Iglesias P, Rubio B (2008) The degree of trace metal pyritization in subtidal sediments of a mariculture area: application to the assessment of toxic risk. Mar Pollut Bull 56:973–983

Álvarez-Iglesias P, Rubio B (2009) Redox status and heavy metal risk in intertidal sediments in NW Spain as inferred from the degrees of pyritization of iron and trace elements. Mar Pollut Bull 58:542–551

Álvarez-Iglesias P, Rubio B, Pérez-Arlucea M (2006) Reliability of subtidal sediments as "geochemical recorders" of pollution input: San Simón Bay Ria de Vigo. NW Spain Estuarine Coast Shelf Sci 70:507–521

Álvarez-Iglesias P, Andrade A, Rey D, Quintana B, Bernabeu AM, López-Pérez AE, Rubio B (2020) Assessment and timing of the anthropogenic imprint and fisheries richness in marine sediments from Ria de Muros NW Iberian Peninsula. Quatern Int 566–567:337–356

Álvarez-Iglesias P, Rubio B (2012) Trace metals in shallow marine sediments from the Ria de Vigo: sources, pollution, speciation and early diagenesis. Geochem. Earth's Syst. Process. 185–210.

Álvarez-Salgado XA, Gago J, Miguez BM, Gilcoto M, Perez FF (2000) Surface water of the NW Iberian margin: upwelling on the shelf versus outwelling of upwelled waters from the Rias Baixas. Estuar Coast Shelf Sci 51:821–837

Álvarez-Vázquez MA, Álvarez-Iglesias P, de Uña-Álvarez E, Quintana B, Caetano M, Prego R (2020) Industrial supply of trace elements during the "Anthropocene": a record in estuarine sediments from the Ria of Ferrol NW Iberian Peninsula. Mar Chem 223:103825. https://doi.org/10.1016/j.marchem.2020.103825

Andrade A, Rubio B, Rey D, Álvarez-Iglesias P, Bernabeu AM, Vilas F (2011) Palaeoclimatic changes during the last 3500 years inferred from diagenetical proxies in the sedimentary record of the Ria de Muros NW Spain. Climate Res 48:247–259

Andrade M, Ramalho RS, Pimentel A, Hernández A, Kutterolf S, Sáez A, Benavente M, Raposeiro PM, Giralt S (2021) Unraveling the Holocene eruptive history of Flores Island Azores through the analysis of lacustrine sedimentary records. Front Earth Sci 29 September 2021. https://doi.org/10.3389/feart.2021.738178

Arias AF, Suárez JF, Navas JR, Cerdán FP, Martín JMB (2008) Mapa de Rocas y Minerales Industriales a E. 1:250.000. Instituto Geológico y Minero de España. Xunta de Galicia.

B Chao R, Costa Casais M, Martínez Cortizas A, Pérez Alberti A, Vázquez Paz M (2002) Holocene evolution on Galician coast NW Spain: an example of paraglacial dynamics. Quatern Int 93–94:149–159. https://doi.org/10.1016/s1040-61820200013-7

Bardos P, Spencer KL, Ward RD, Maco BH, Cundy AB (2020) Integrated and sustainable management of post-industrial coasts. Front Environ Sci 8:86. https://doi.org/10.3389/fenvs.2020.00086

Barreiro Lozano R, Carballeira Ocaña A, Real Rodriguez C (1988) Metales pesados en los sedimentos de cinco sistemas de Rias Ferrol, Burgo, Arousa, Pontevedra y Vigo. Thalassas 6:61–70

Barros GV, Martinelli LA, Oliveira Novais TM, Ometto JP, Zuppi GM (2010) Stable isotopes of bulk organic matter to trace carbon and nitrogen dynamics in an estuarine ecosystem in Babitonga Bay Santa Catarina, Brazil. Sci Total Environ 408:2226–2232

Belzunce Segarra MJ, Prego R, Wilson MJ, Bacon J, Santos-Echeandía J (2008) Metal speciation in surface sediments of the Vigo Ria NW Iberian Peninsula. Sci Mar 72:119–126

Bern CR, Walton-Day K, Naftz DL (2019) Improved enrichment factor calculations through principal component analysis: examples from soils near breccia pipe uranium mines, Arizona, USA. Environ Pollut 248:90–100

Bernárdez P, González-Álvarez R, Francés G, Prego R, Bárcena MA, Romero OE (2008) Late Holocene history of the rainfall in the NW Iberian Peninsula—evidence from a marine record. J Mar Syst 721–4:366–382

Berner RA (1983) Sedimentary pyrite formation, an update. Geochemica Et Cosmochimica Acta 48:605–615

Bhatia MR, Crook KA (1986) Trace element characteristics of graywackes and tectonic setting discrimination of sedimentary basins. Contrib Miner Petrol 922:181–193

Bianchi GG, Mccave IN (1999) Holocene periodicity in North Atlantic climate and deep-ocean flow south of Ice-land. Nature 397:515–517. https://doi.org/10.1038/17362

Bijan Noori B, Ghadimvand NK, Movahed B, Yousefpour M (2016) Provenance and Tectonic setting of Late Lower Cretaceous Albian Kazhdumi Formation sandstones SW Iran. Open Journal of Geology 6:721–739. https://doi.org/10.4236/ojg.2016.68055

Birch GF (2017) Determination of sediment metal background concentrations and enrichment in marine environments—a critical review. Sci Total Environ 580:813–831

Bouchet VMP, Frontalini F, Francescangeli F, Sauriau P-G, Geslin E, Martins MVA, Almogi-Labin A, Avnaim-Katav S, Di Bella L, Cearreta A, Coccioni R, Costelloe A, Dimiza MD, Ferraro F, Haynert K, Martínez-Colón M, Melis R, Schweizer M, Triantaphyllou MV, Tsujimoto A, Wilson B, Armynot du Châtelet E (2021) Indicative value of benthic foraminifera for biomonitoring: assignment to ecological groups of sensitivity to total organic carbon of species from European intertidal areas and transitional waters. Mar Pollut Bull 164:112071. https://doi.org/10.1016/j.marpolbul.2021.112071

Bronk Ramsey C (2001) Development of the radiocarbon calibration program OxCal. Radiocarbon 43(2A):355–363

Bronk Ramsey C (2008) Deposition models for chronological records. Quatern Sci Rev 27(1–2):42–60

Bronk Ramsey C (2009) Bayesian analysis of radiocarbon dates. Radiocarbon 511:337–360

Bronk Ramsey C (2010) OxCal v4.1.7 https://c14.arch.ox.ac.uk/login/login.php?Location=/oxcal/ OxCal.html

Buat-Menard P, Chesselet R (1979) Variable influence of the atmospheric flux on the trace metal chemistry of oceanic suspended matter. Earth Planet Sci Lett 42:398–411. https://doi.org/10.1016/0012-821X7990049-9

Bueno C, Figueira R, Ivanoff MD, Toldo Junior EE, Fornaro L, García-Rodríguez FG (2019) A multi proxy assessment of long–term anthropogenic impacts in Patos Lagoon, southern Brazil. Journal of Sedimentary Environments 4(3):276–290

Bury JB (2005) A History of the Later Roman Empire from Arcadius to Irene 395 A.D. to 800 A.D. Adamant Media Corp. ISBN 978–1402183683.

Canário J, Prego R, Vale C, Branco V (2007) Distribution of mercury and monomethylmercury in sediments of Vigo Ria, NW Iberian Peninsula. Water Air Soil Pollut 182:21–29

Canosa F, Martin-Izard A, Fuertes-Fuente M (2012) Evolved granitic systems as a source of rare element deposits: The Ponte Segade case Galicia, NW Spain. Lithos 153:165–176

Carballeira A, Carral E, Puente XM, Villares R (19970 Estado de Conservacion de la Costa de Galicia. Nutrientes y Metales pesados en sedimentos y organismos intermareales. Universidad de Santiago de Compostela. Xunta de Galicia, Conselleria de Pesca, Marisqueo y Acuicultura, pp. 107.

Carral E, Villares R, Puente X, Carballeira A (1995) a. Influence of watershed lithology on heavy metal levels in estuarine sediments and organisms in Galicia north-west Spain. Mar Pollut Bull 30:604–608

Carral E, Puente X, Villares R, Carballeira A (1995) b. Background heavy metal levels in estuarine sediments and organisms in Galicia northwest Spain as determined by modal analysis. Sci Total Environ 172:175–188

Carranza EJM (2017) Geochemical mineral exploration: should we use enrichment factors or log-ratios? Nat Resour Res 26(4):411–428. https://doi.org/10.1007/s11053-016-9318-z

Carrión Y, Kaal J, López-Sáez JA, López-Merino L, Martínez Cortizas A (2010) Holocene vegetation changes in NW Iberia revealed by anthracological and palynological records from a colluvial soil. The Holocene 20:53–66. https://doi.org/10.1177/0959683609348849

Cepedal A, Fuertes-Fuente M, Martín-Izard A, Barrero M (2008) Gold-bearing As-rich pyrite and arsenopyrite from the El Valle gold deposit, Asturias, northwestern Spain. Can Mineral 461:233–247. https://doi.org/10.3749/canmin.46.1.233

Cepedal A, Fuertes-Fuente M, Martin-Izard A, García-Nieto J, Boiron MC (2013) J Geochem Explor 124:101–126.https://doi.org/10.1016/j.gexplo.2012.08.010

Cetecioğlu Z, Ince BK, Kolukirik M, Ince O (2009) Biogeographical distribution and diversity of bacterial and archaeal communities within highly polluted anoxic marine sediments from the Marmara Sea. Mar Pollut Bull 58(3):384–395

Chen G, Robertson AHF (2020) User's guide to the interpretation of sandstones using whole-rock chemical data, exemplified by sandstones from Triassic to Miocene passive and active margin

settings from the Southern Neotethys in Cyprus. Sed Geol 400:105616. https://doi.org/10.1016/j.sedgeo.2020.105616
Claude D (1987) Término municipal: Plasenzuela, in Catalogue des mines et des fonderies antiques de la Peninsule Iberique: Publications de la Casa de Velazquez, serie archeologie, Fac. VIII, t 1:53–57
Comendador Rey BC, Meunier E, Figueiredo E, Lackinger A, Fonte J et al (2016) Northwestern Iberian tin mining from bronze age to modern times: an overview. a celebration of the tin working landscape of Dartmoor in its European context: Prehistory to 20th century, Dartmoor Tin working Research Group, May 2016, Tavistock, United Kingdom. pp.133–153.
Condie KC (1993) Chemical composition and evolution of the upper continental crust: contrasting results from surface samples and shales. Chem Geol 1041–4:1–37
Cullers RL (2002) Implications of elemental concentrations for provenance, redox conditions, and metamorphic studies of shales and limestones near Pueblo, CO, USA. Chem Geol 1914:305–327
Cullers RL, Podkovyrov VN (2000) Geochemistry of the Mesoproterozoic Lakhanda Shales in Southeastern Yakutia, Russia: Implications for Mineralogical and Provenance Control, and Recycling. Precambr Res 104:77–93. https://doi.org/10.1016/S0301-9268(00)00090-5
Davies-Colley RJ, Nelson PO, Williamson KJ (1985) Sulfide control of cadmium and copper concentrations in anaerobic estuarine sediments. Mar Chem 16:173–186
de Blas MA (1996) La primera mineria metálica del N. Peninsular: las indicaciones del C-14 y la cronología prehistórica de las explotaciones del Aramo y el Milagro. Complutum extra 217–266.
de Blas MA (2005) Un témoignage probant de l'exploitation préhistorique du cuivre dansle nord de la péninsule ibérique: le complexeminier de l'Aramo.Mém. S. Préhist., F 37, 195–205.
Debenay J-P, Guillou J-J (2002) Ecological Transitions Indicated by Foraminiferal Assemblages in Parlic Environments. Estuaries, 25 6, Part A, 1107–1120.
Deines P (1980) The isotopic composition of reduced organic carbon. In: P. Fritz and J.C.H. Fontes eds., Handbook of Environmental Isotope Geochemistry. Elsevier Scientific Publishing Company, Amsterdam, vol. 1, pp. 329–406.
Dias da Silva I, Fernández RD, Díez-Montes A, Clavijo EG, Foster DA (2016) Magmatic evolution in the N-Gondwana margin related to the opening of the Rheic Ocean - evidence from the Upper Parautochthon of the Galicia-Trás-os-Montes Zone and from the Central Iberian Zone NW Iberian Massif. Int J Earth Sci Geol Rundsch 105:1127–1151. https://doi.org/10.1007/s00531-015-1232-9
Díez Fernández R, Martínez Catalán JR, Arenas R, Abati J, Gerdes A, Fernández-Suárez J (2012) U-Pb detrital zircon analysis of the lower allochthon of NW Iberia: age constraints, provenance and links with the Variscan mobile belt and Gondwanan cratons. J Geol Soc 169:655–665
Diz P, Francés G, Pelejero C, Grimalt JO, Vilas F (2002) The last 3000 years in the Rı ´a de Vigo NW Iberian Margin: climatic and hydrographic signals. Holocene 12(4):459–468
Duarte LM (1995) A atividade mineira em Portugal durante a Idade Média: tentativa de síntese". Revista da Faculdade de Letras. Porto: Faculdade de Letras da Universidade do Porto, 12, 75–112.
Duleba W, Teodoro AC, Debenay J-P, Alves Martins MV, Gubitoso S, Pregnolato LA, Lerena LM, Prada SM, Bevilacqua JE (2018) Environmental impact of the largest petroleum terminal in SE Brazil: a multiproxy analysis based on sediment geochemistry and living benthic foraminifera. PLoS ONE 132:e0191446. https://doi.org/10.1371/journal.pone.0191446
Duleba W, Gubitoso S, Alves Martins MV, Teodoro AC, Pregnolato LA, Prada SM (2019) Evaluation of contamination by potentially toxic elements PTE of sediments around the petroleum terminal pipeline "Dutos e Terminais do Centro Sul DTCS", SP, Brazil. J Sediment Environ 4(4):387–402. https://doi.org/10.12957/jse.2019.46539
Emslie SD, Brasso R, Patterson WP, Carlos Valera A, McKenzie A, Maria Silva A, Gleason JD, Blum JD (2015) Chronic mercury exposure in Late Neolithic/Chalcolithic populations in Portugal from the cultural use of cinnabar. Sci Rep 5:14679. https://doi.org/10.1038/srep14679
Emslie SD, Alderman A, McKenzie A, Brasso R, Taylor AR, Molina Moreno M, Cambra-Moo O, González Martín A, Silva AM, Valera A, García Sanjuán L, Vijande Vila E (2019) Mercury in archaeological human bone: biogenic or diagenetic? J Archaeol Sci 108:104969. https://doi.org/10.1016/j.jas.2019.05.005
Evans G, Howard RJ, Nombela MA (2003) Metals in the sediments of Ensenada de San Simón inner Ria de Vigo, Galicia, NW Spain. Appl Geochem 18:983–996
Farias P, Ordoñez-Casado B, Marcos A, Rubio-Ordoñez A, Fanning CM (2014) U-Pb zircon SHRIMP evidence for Cambrian volcanism in the Schistose Domain within the Galicia–Trás–os–Montes Zone Variscan Orogen. NW Iberian Peninsula Geologica Acta 12(3):209–218. https://doi.org/10.1344/GeologicaActa4.12.3.3
Figueiredo E, Fonte J, Lima A, Veiga JP, Silva RJC, Mirão J (2018) Ancient tin production: slags from the Iron Age Carvalhelhos hillfort NW Iberian Peninsula. J Archaeol Sci 93:1–16
Fiúza AFG (1983) Upwelling patterns off Portugal. In: Suess E, Thiede J (eds) Coastal upwelling its sediment record. Plenum Press, New York, pp 85–98
Fiúza AFG et al (1982) Climatological space and time variation of the Portuguese coastal upwelling. Oceanol Acta 5:31–40
Floor P (1966) Petrology of an aegirine-riebeckite gneiss-bearing part of the Hesperian massif: The Galiñeiro and surrounding areas. Leidse Geologische Mededelingen, 36, Vigo, Spain. 204 pp.
Floyd P, Leveridge B (1987) Tectonic environment of the Devonian Gramscatho basin, south Cornwall: framework mode and geochemical evidence from turbiditic sand-stones. J Geol Soc 144:531–542
Folk RL, Ward WC (1957) Brazos River bar: a study in the significance of grain size parameters. J Sediment Petrol 27:3–26. https://doi.org/10.1306/74D70646-2B21-11D7-8648000102C1865D
Fraga, F., Margalef, R., 1979. Las Rias gallegas. In Universidad de Santiago, editor, Estudio y Explotación del Mar en Galicia, La Coruña, 245–98.
Fuente MF, Izard AM (1994) El campo pegmatítico de Forcarey y las mineralizaciones de Sn, Ta, y Nb asociadas Pontevedra, Galicia. España. Boletín De La Sociedad Española De Mineralogía 17:51–63
Fuertes-Fuente M, Martin-Izard A (1994) El campo pegmatítico de Forcarey y las mineralizaciones de Sn, Ta, y Nb asociadas Pontevedra, Galicia. España. Boletín De La Sociedad Española De Mineralogía 17:51–63
Fuertes-Fuente M, Martin-Izard A, Boiron MC, Mangas J (2000) Fluid evolution of rare-element and muscovite granitic pegmatites from central Galicia, NW Spain. Miner Depos 35:332–345
García-García A, García-Gil S, Vilas F (1999) A seeping sea–floor in a Ria environment: Ria de Vigo NW Spain. Environ Geol 38(4):296–300
García-García A, García-Gil S, Vilas F (2005) Quaternary evolution of the Ria de Vigo, Spain. Mar Geol 220:153–179. https://doi.org/10.1016/j.margeo.2005.06.015
Gasteiger J, Groß S, Freudenthaler V, Wiegner M (2011) Volcanic ash from Iceland over Munich: mass concentration retrieved from ground-based remote sensing measurements. Atmos Chem Phys 11:2209–2223. https://doi.org/10.5194/acp-11-2209-2011

Gebregiorgis D, Giosan L, Hathorne EC, Anand P, Nilsson-Kerr K, Plass A (2020) What can we learn from X-ray fluorescence core scanning data? A paleomonsoon case study. Geochem Geophys Geosyst 21:2019GC008414. https://doi.org/10.1029/2019GC008414

Gil-Ibarguchi JI, Ortega E (1985) Petrology, structure and geotectonic implications of glaucophane-bearing eclogites and related rocks from the Malpica-Tuy MT unit, Galicia, northwest Spain. In: D.C. Smith, G. Franz and D. Gebauer Guest-Editors, Chemistry and Petrology of Eclogites. Chem. Geol., 50, 145–162.

Gil-lbarguchi JI (1994) Petrology of jadeite metagranite and associated orthogneiss from the Malpica-Tuy allochthon Northwest Spain. Eur. J. Mineral.

Giradeau J et al (2000) Coccolith evidence for instabilities in surface circulation south of Iceland during Holocene times, Earth Planet. Sci 179:257–268

González Álvarez R, Bernárdez P, Pena LD, Francés G, Prego R, Diz P, Vilas F (2005) Paleoclimatic evolution of the Galician continental shelf NW of Spain during the last 3000 years: from a storm regime to present conditions. J Mar Syst 541–4:245–260

Grousset FE, Cortijo E, Huon S, Hervé L (2001) Zooming in on Heinrich layers. Paleoceanography 16:240–259

Gudmundsson MT, Thordarson T, Höskuldsson A, Larsen G, Björnsson H, Prata FJ, Oddsson B, Magnússon E, Högnadóttir T, Petersen GN, Hayward CL, Stevenson JA, Jónsdóttir I (2012) Ash generation and distribution from the April–May 2010 eruption of Eyjafjallajökull, Iceland. Sci Rep-UK 2:572. https://doi.org/10.1038/srep00572

Gutiérrez Claverol M, Martínez García E, Luque C, Suárez V, Ruiz F (1991) Gold deposits, Late Hercynian tectonics and magmatism in the northeastern Iberian Massif NW Spain. Chron Rech Minière 503:3–13

Hallam A (1971) Mesozoic Geology and the Opening of the North Atlantic. J Geol 79(2):129–157. https://www.jstor.org/stable/30079724

Hastings DW, Schwing PT, Brooks GR, Larson RA, Morford JL, Roeder T, Quinn KA, Bartlett T, Romero IC, Hollander DJ (2016) Changes in sediment redox conditions following the BP DWH blowout event. Deep-Sea Res II 129:167–178. https://doi.org/10.1016/j.dsr2.2014.12.009

Hemming SR (2004) Heinrich events: massive late Pleistocene detritus layers of the North Atlantic and their global impact. Review of Geophysics, 42, RG1005. Paper number 2003RG000128, 43 pp.

Hensen BJ (1967) Mineralogy and petrography of some tin, lithium and beryllium bearing albite pegmatites near Doade, Galicia. Spain Leidse Geol Med 39:249–259

Hillman AL, Abbott MB, Valero-Garcés BL, Morellon M, Barreiro-Lostres F, Bain DJ (2017) Lead pollution resulting from Roman gold extraction in northwestern Spain. The Holocene 2710:1465–1474

Hong S, Candelone J-P, Patterson CC, Boutron CF (1994) Greenland ice evidence of hemispheric lead pollution two millennia ago by Greek and Roman civilizations. Science 265:1841–1843

Hong S, Candelone J-P, Patterson CC, Boutron CF (1996) History of ancient copper smelting pollution during Roman and Medieval times recorded in the Greenland ice. Science 272:246–249

Hossain HZ, Kawahata H, Roser BP, Sampei Y, Manaka T, Otani S (2017) Geochemical characteristics of modern river sediments in Myanmar and Thailand: implications for provenance and weathering. Geochemistry 773:443–458

Hurrell JW (1995) Decadal trends in the North Atlantic Oscillation: regional temperatures and precipitation. Science 269:679

Hurrell JW et al (2001) The North Atlantic Oscillation. Science 291(5504):603

Iglésias M, Ribeiro ML, Ribeiro A (1983) La interpretación aloctonista de la estructura del noroeste peninsular. Comba. J.A. Coord. - Libro Jubilar de J.M. Rios. Tomo I. Instituto Geológico y Minero de España, Madrid, pp 459–467

Irabien MJ, Cearreta A, Urteaga M (2012) Historical signature of Roman mining activities in the Bidasoa estuary Basque Country, northern Spain: an integrated micropalaeontological, geochemical and archaeological approach. J Archaeol Sci 39:2361–2370. https://doi.org/10.1016/j.jas.2012.02.023

Irabien MJ, Cearreta A, Gómez-Arozamena J, García-Artola A (2020) Holocene vs Anthropocene sedimentary records in a human-altered estuary: The Pasaia case northern Spain. Mar Geol 429:106292. https://doi.org/10.1016/j.margeo.2020.106292

Jahoda C, Andrews J, Foster R (1989) Structural controls of Monte Roso and other gold deposits in NW Spain fractures jogs and hot-jogs. Trans Inst Mining Metall B 98:1–6

Jørgensen BB, Findlay AJ, Pellerin A (2019) The Biogeochemical Sulfur Cycle of Marine Sediments. Front Microbiol 10:849. https://doi.org/10.3389/fmicb.2019.00849

Jouanneau JM, Weber O, Drago T, Rodrigues A, Oliveira A, Dias JMA, Reyss JL (2002) Recent sedimentation and sedimentary budgets on the western Iberian shelf. Prog Oceanogr 522–4:261–275

Julivert M, Fontbote JM, Ribeiro A, Conde L (1980) Mapa tectonico de la Península Ibérica y Baleares scale 1/1 000 000 — explicative memory. Institute Geologico y Geominero de España, Madrid

Kaal J, Marco YC, Asouti E, Seijo MM, Martínez Cortizas A, Casáis MC, Boado FC (2011) Long-term deforestation in NW Spain: linking the Holocene fire history to vegetation change and human activities. Quatern Sci Rev 30:161–175. https://doi.org/10.1016/j.quascirev.2010.10.006

Kabata-Pendias A, Pendias H (1992) Trace Elements in Soils and Plants, 2nd edn. CRC Press, Boca Raton

Killick D, Fenn T (2012) Archaeometallurgy: the study of preindustrial mining and metallurgy. Annu Rev Anthropol 41:559–575

Kylander ME, Weiss DJ, Martínez-Cortizas A, Spiro B, Garcia-Sanchez R, Coles BJ (2005) Refining the pre-industrial atmospheric Pb isotope evolution curve in Europe using an 8000 years old peat core from NW Spain. Earth Planet Sci Lett 240:467–485. https://doi.org/10.1016/j.epsl.2005.09.024

Lage MOP (2020) In the memories of Wolfram - a Portuguese-Galician Sociolect. Int J Human Soc Sci Educ IJHSSE, 7(7):124–134. https://doi.org/10.20431/2349-0381.0707015

Lamb AL, Wilson GP, Leng MJ (2006) A review of coastal palaeoclimate and relative sea–level reconstructions using $\delta^{13}C$ and C/N ratios in organic material. Earth Sci Rev 75:29–57. https://doi.org/10.1016/j.earscirev.2005.10.003

Leblanc M, Morales JA, Borrego J, Elbaz-Poulichet F (2000) 4,500-Year-old mining pollution in Southwestern Spain: long-term implications from modern mining pollution. Econ Geol 95(3):655–662. https://doi.org/10.2113/gsecongeo.95.3.655

Licht OAB, Plawiak RAB (2005) Projeto Geoquímica de Solos, Horizonte B: levantamento geoquímico multielementar do Estado do Paraná: relatório final. MINEROPAR, Curitiba, 2, 408 p.

Lima A, Matias Rodríguez R, Félix N & Silva, MA (2011) A Mineração Romana de ouro no Município de Paredes: o exemplo da Serra de Santa Iria e Serra das Banjas. In: Actas do VI Simpósio sobre Mineração e Metalurgia Históricas no Sudoeste Europeu (Vila Velha do Ródão - 2010). Abrantes, pp 125–142

Lin CY, Turchyn AV, Krylov A, Antler G (2020) The microbially driven formation of siderite in salt marsh sediments. Geobiology 18:207–224. https://doi.org/10.1111/gbi.12371

Llera AR, Fuertes-Fuente M, Cepedal A, Martin-Izard A (2019) Barren and Li–Sn–Ta mineralized pegmatites from NW Spain Central Galicia: a comparative study of their mineralogy, geochemistry, and wallrock metasomatism. Minerals 9:739. https://doi.org/10.3390/min9120739

López-Carmona A, Pitra P, Abati J (2013) Blueschist-facies metapelites from the Malpica-Tui Unit NW Iberian Massif: phase equilibria

modelling and H_2O and Fe_2O_3 influence in high-pressure assemblages. J Metamorph Geol 31:263–280

López-Costas O, Kylander M, Mattielli N, Álvarez-Fernández N, Pérez-Rodríguez M, Mighall T, Bindler R, Martínez Cortizas A (2020) Human bones tell the story of atmospheric mercury and lead exposure at the edge of Roman World. Sci Total Environ 710(2020):136319. https://doi.org/10.1016/j.scitotenv.2019.136319

López-Merino L, Silva Sánchez N, Kaal J, López-Sáez JA, Martínez Cortizas A (2012) Post-disturbance vegetation dynamics during the Late Pleistocene and the Holocene: an example from NW Iberia. Global Planet Change 92–93:58–70. https://doi.org/10.1016/j.gloplacha.2012.04.003

López-Merino L, Martínez Cortizas A, Reher GS, López-Sáez JA, Mighall TM, Bindler R (2014) Reconstructing the impact of human activities in a NW Iberian Roman mining landscape for the last 2500 years. J Archaeol Sci 50:208–218

Macías F, Calvo de Anta R (2008) Niveles Genéricos de Referencia de Metales Pesados y Otros Elementos Traza en Suelos de Galicia; Consellería de Medio Ambiente e Desenvolvemento Sostible: Santiago de Compostela, Spain.

Magurran AE (1988) Ecological Diversity and Its Measurement. University Press, Princeton, NJ

Marmolejo-Rodríguez AJ, Caetano M, de Pablo H, Vale C, Prego R (2008) Yttrium in the Vigo Ria NW Iberian Peninsula: sources, distribution, and background levels. Cienc Mar 34(3):399–406

Martinelli LP, Ometto JPHB, Ferraz ES, Victoria RL, Camargo PB. Moreira MZ (2009) Desvendando questões ambientais com isótopos estáveis [Unraveling environmental issues with stable isotopes]. Oficina de Textos, São Paulo.

Martínez Catalán JR, Gómez Barreiro J, Dias da Silva Í, Chichorro M, López-Carmona A, Castiñeiras P, Abati J, Andonaegui P, Fernández-Suárez J, González Cuadra P, Benítez-Pérez JM (2019) Variscan suture zone and suspect terranes in the NW Iberian Massif: allochthonous complexes of the Galicia-Trás os Montes Zone NW Iberia. In: Quesada, C. and Oliveira, J.T. eds., The geology of Iberia: a geodynamic approach, vol. 2, Springer Nature Switzerland, Cham, pp. 99–130.

Martínez Cortizas A, Pontevedra Pombal X, Novoa Munoz JC, García-Rodeja E (1997) Paleocontaminacion: evidencias de contaminacion atmosferica en Galicia durante los ultimos 4000 anos. Gallaecia 16:7–22

Martínez Cortizas A, Peiteado Varela E, Bindler R, Biester H, Cheburkin A (2012) Reconstructing historical Pb and Hg pollution in NW Spain using multiple cores from the Chao de Lamoso bog Xistral Mountains. Geochimica Cosmochimica Acta 82:68–78

Martínez Cortizas A, López-Merino L, Bindler R, Mighall T, Kylander ME (2016) Early atmospheric metal pollution provides evidence for Chalcolithic/Bronze Age mining and metallurgy in southwestern Europe. Sci Total Environ 545:398–406

Martínez Cortizas A, López-Costas O, Orme L, Mighall T, Kylander ME, Bindler R, Sala AG (2020) Holocene atmospheric dust deposition in NW Spain. The Holocene 304:507–518. https://doi.org/10.1177/0959683619875193

Martinez Cortizas A, Pontevedra-Pombal X, Garcia-Rodeja E, Novoa-Munoz JC, Shotyk W (1999) b. Mercury in a Spanish peat bog: archive of climate change and atmospheric metal deposition. Science 284:939–942

Martinez Cortizas A, Mighall T, Pontevedra Pombal X, Novoa Munfoz JC, Peiteado Varelal E, Piñeiro Rebolo R (2005) Linking changes in atmospheric dust deposition, vegetation change and human activities in northwest Spain during the last 5300 years. The Holocene 15:698–706. https://doi.org/10.1191/0959683605hl834rp

Martínez-Abad I, Cepedal A, Arias D, Martín-Izard A (2015) The Vilalba gold district, a new discovery in the Variscan terranes of the NW of Spain: a geologic, fluid inclusion and stable isotope study. Ore Geol Rev 66:344–365. https://doi.org/10.1016/j.oregeorev.2014.10.021

Martínez-Cortizas A, Pontevedra-Pombal X, Nóvoa Muños JC, García-Rodeja E (1997) Four thousand years of atmospheric Pb, Cd and Zn deposition recorded by the ombrotrophic peat bog of Penido Vello Northwestern Spain. Water, Air, and Soil Pollut 100:387–403

Martínez-Cortizas A, Garcia-Rodeja E, Pombal XP, Munoz JC, Weiss D, Cheburlin A (2002) Atmospheric Pb deposition in Spain during the last 4600 years recorded by two ombrotrophic peat bogs and implications for the use of peat as archive. Sci Total Environ 292:33–44. https://doi.org/10.1016/S0048-96970200031-1

Martínez-Cortizas A, López-Merino L, Bindler R et al (2013) Atmospheric Pb pollution in N Iberia during the Late Iron Age/Roman times reconstructed using the high-resolution record of La Molina mire Asturias, Spain. J Paleolimnol 50:71–86

Martínez Cortizas A, Pontevedra Pombal X, Novoa Munoz JC, García-Rodeja E (1997b) Paleocontaminacion: evidencias de contaminacion atmosferica en Galicia durante losultimos 4000 anos. Gallaecia 16:7–22

Martins V, Dubert J, Jouanneau J-M, Weber O, Silva EF, Patinha C, Alveirinho Dias JM, Rocha F (2007) A multiproxy approach of the Holocene evolution of shelf–slope circulation on the NW Iberian Continental Shelf. Mar Geol 239:1–18. https://doi.org/10.1016/j.margeo.2006.11.001

Martins V, Abrantes I, Grangeia C, Martins P, Nagai R, Sousa SHM, Laut LLM, Alveirinho Dias JM, João M, da Silva EF, Rocha F (2012) Records of sedimentar dynamics in the continental shelf and upper slope between Aveiro-Espinho N Portugal. J Mar Syst 96:48–60. https://doi.org/10.1016/j.jmarsys.2012.02.001

Martins V, Rocha F, Sequeira C, Martins P, Santos J, Dias JA, Weber O, Jouanneau J-M, Rubio B, Rey D, Bernabeu A, Silva E, Laut L, Figueira R (2013) Late Holocene climatic oscillations traced by clay mineral assemblages and other paleoceanographic proxies in Ria de Vigo NW Spain. Turkish Journal of Earth Sciences 22:398–413. https://doi.org/10.3906/yer-1112-12

Martins V, Santos JF, Mackensen A, Dias JM, Ribeiro S, Moreno J, Soares AM, Frontalini F, Rey D, Rocha F (2013) The sources of the glacial IRD in the NW Iberian Continental Margin over the last 40 ka. Quatern Int 318:128–138. https://doi.org/10.1016/j.quaint.2013.08.026

Martins MVA, Dias JMA, Mane MÂ, Rocha F (2016) Geochemical fingerprints of climatic oscillations during the Late Holocene in Ria de Vigo N Spain. J Sediment Environ 11:78–89

Martins MVA, Rey D, Pereira E, Plaza-Morlote M, Salgueiro E, Moreno J, Duleba W, Ribeiro S, Santos JF, Bernabeu A, Rubio B, Laut LLM, Frontalini F, Conceição Rodrigues MAC, Rocha F (2018) Influence of dominant wind patterns in a distal region of the NW Iberian Margin during the last glaciation. J Geol Soc London 175:321–335. https://doi.org/10.1144/jgs2017-075

Martins MVA, Hohenegger J, Frontalini F, Alveirinho Dias JM, Geraldes MC, Rocha F (2019) Dissimilarity between living and dead benthic foraminiferal assemblages in the Aveiro Continental Shelf Portugal. PLoS ONE 141:e0209066. https://doi.org/10.1371/journal.pone.0209066

McLennan SM, Hemming S, McDaniel DK, Hanson GN (1993) Geochemical approaches to sedimentation, provenance, and tectonics. Special Papers–Geological Society of America, 21–21.

Méndez G, Vilas F (2005) Geological antecedents of the Rias Baixas Galicia, northwest Iberian Peninsula. J Mar Syst 541–4:195–207

Meunier E (2011) L'exploitation de l'étain dans le Nord-Ouest ibérique entre l'Age du Bronze et la fin de l'Empire romain: bilan et perspectives. Master Thesis, University of Toulouse. Unpublished

Meyers PA (1997) Organic geochemical proxies of paleoceanographic, paleolimnological, paleoclimatic processes. Organic Geochemistry, Oxford 27:213–250

Mighall TM, Martínez Cortizas A, Biester H, Turner SE (2006) Proxy climate and vegetation 467 changes during the last five millennia in NW Iberia: pollen and non-pollen palynomorph data from two ombrotrophic peat bogs in the North Western Iberian Peninsula. Rev Palaeobot Palynol 141:203–223. https://doi.org/10.1016/j.revpalbo.2006.03.013

Montero P, Floor P, Corretgé G (1998) The accumulation of rare-earth and high field strength elements in peralkaline granitic rocks: the Galiñeiro orthogneissic complex, northwestern Spain. The Canadian Mineralogist. J. Mineral. Assoc. Canada 35:683–700

Montero P, Bea F, Corretgé LG, Floor P, Whitehouse MJ (2009) U-Pb ion microprobe dating and Sr and Nd isotope geology of the Galiñeiro Igneous Complex. A model for the peraluminous/peralkaline duality of the Cambro-Ordovician magmatism of Iberia. Lithos 107:227–238

Moore RB (1990) Volcanic geology and eruption frequency, Silo Miguel, Azores. Bull Volcanol 52:602–614. https://doi.org/10.1007/BF00301211

Muhly JD (1973) Copper and tin: the distribution of mineral resources and the nature of the metals trade in the Bronze Age. Trans Conn Acad Arts Sci 43:155–535

Muhly JD (1988) The beginnings of metallurgy in the Old World. See Maddin 1988:2–20

Müller VG (1986) Schadstoffe in Sedimenten – Sedimente als Schadstoffe. Mitteilungen Der Österreichischen Geologischen Gesellschaft 79:107–126

Murad E (1978) Yttrium and zirconium as geochemical guide elements in soil and stream sediment sequences. Eur J Soil Sci 29:219–223

Nace TE, Baker PA, Dwyer GS, Silva CG, Rigsby CA, Burns SJ, Giosan L, Otto-Bliesner B, Liu Z, Zhu J (2014) The role of North Brazil current transport in the paleoclimate of the Brazilian Nordeste margin and paleoceanography of the western tropical Atlantic during the late Quaternary. Palaeogeogr Palaeoclimatol Palaeoecol. https://doi.org/10.1016/j.palaeo.2014.05.030

Nombela MA, Vilas F, Evans G (1995) Sedimentation in the mesotidal Rias Bajas of Galicia north-western Spain: Ensenada de San Simón, inner Ria de Vigo. Spec Publ Int Assoc Sedimentol 24:133–149

Nriagu JO (1979) Global inventory of natural and anthropogenic emissions of trace metals to the atmosphere. Nature 279:409–411

Nriagu JO (1983) Lead and lead poisoning in Antiquity. Willey, New York

O'Brien W (2015) Prehistoric copper mining in Europe, 5500–500 BC. Oxford University Press, Oxford and New York

Okunlola OA, Idowu O (2012) The geochemistry of claystone–shale deposits from the Maastritchian Patti formation, Southern Bida basin, Nigeria. Earth Sci Res J 162:139–150

Olid C, García-Orellana J, Martínez-Cortizas A, Masqué P, Peiteado-Varela E, Sanchez-Cabeza J-A (2010) Multiple site study of recent atmospheric metal Pb, Zn and Cu deposition in the NW Iberian Peninsula using peat cores. Sci Total Environ 408:5540–5549. https://doi.org/10.1016/j.scitotenv.2010.07.058

Olid C, García-Orellana J, Masqué P et al (2013) Improving the 210Pb-chronology of Pb deposition in peat cores from Chao de Lamoso NW Spain. Sci Total Environ 443:597–607

Orejas A, Sánchez-Palencia FJ (2002) Mines, Territorial organization, and social structure in Roman Iberia: Carthago Noua and the Peninsular Northwest. Am J Archaeol 106(4):581–599. https://doi.org/10.2307/4126218

Parga-Pondal I, Cardoso GM (1948) Die Lithiumpegmatite von Lalin in Galizien. Prov. Pontevedra. Spanien Schweiz Min Petr Mitt 28:324–334

Pazos O, Nombela MA, Vilas F (2000) Continental contribution of suspended sediment to an estuary: Ria de Vigo. Sci Mar 64(3):295–302

Penhallurick RD (1986) Tin in antiquity: its mining and trade throughout the Ancient World with particular reference to Cornwall. IOM Communications Ltd, London

Perez-Arlucea M, Mendez G, Clemente F, Nombela M, Rubio B, Filgueira M (2005) Hydrology, sediment yield, erosion and sedimentation rates in the estuarine environment of the Ria de Vigo, Galicia, Spain. J Mar Syst 54:209–226

Pérez-García LC, Sanchez-Palencia FJ, Torres-Ruiz J (2000) Tertiary and Quaternary alluvial gold deposits of Northwest Spain and Roman mining NW of Duero and Bierzo Basins. J Geochem Explor 71:225–240

Pérez-López M, Méndez García M, Alonso Díaz J, Melgar Riol MJ (2004) Evolución temporal de la contaminación por plomo y cadmio en la zona intermareal de la Ría de Vigo. Revista Salud Ambiental 4:21–24

Piedracoba S, Álvarez-Salgado XA, Rosón G, Herrera JL (2005) Short-timescale thermohaline variability and residual circulation in the central segment of the coastal upwelling system of the Ria de Vigo northwest Spain during four contrasting periods. J Geophys Res C Ocean 110:1–15. https://doi.org/10.1029/2004JC002556

Piering ED, Pevida LR, Maldonado C, González S, García J, Varela A, Arias D, Martin-Izard A (2000) The gold belts of western Asturias and Galicia NW Spain. J Geochem Explor 71:89–101

Plaza Morlote M, Rey D, Santos JF, Ribeiro S, Heslop D, Bernabeu AM, Mohamed KJ, Rubio B, Martins V (2017) Southernmost evidence of large European Ice Sheet-derived freshwater discharges during the Heinrich Stadials of the Last Glacial Period Galician Interior Basin, Northwest Iberian Continental Margin. Earth Planet Sci Lett 457:213–226

Pontevedra-Pombal X, Mighall TM, Nóvoa-Muñoz JC, Peiteado-Varela E, Rodríguez-Racedo J, García-Rodeja E, Martínez-Cortizas A (2013) Five thousand years of atmospheric Ni, Zn, As, and Cd deposition recorded in bogs from NW Iberia: prehistoric and historic anthropogenic contributions. J Archaeol Sci 40(1):764–777. https://doi.org/10.1016/j.jas.2012.07.010

Prego R (1993) General aspects of carbon biogeochemistry in the Ria of Vigo, northwestern Spain. Geochim Cosmochim Acta 57:2041–2052

Prego R, Cobelo-Garcia A (2003) Twentieth century overview of heavy metals in the Galician Rias NW Iberian Peninsula. Environ Pollut 121:425–452

Radivojević M, Roberts BW, Pernicka E et al (2019) The provenance, use, and circulation of metals in the European Bronze Age: the state of debate. J Archaeol Res 27:131–185. https://doi.org/10.1007/s10814-018-9123-9

Rahman MM, Alam K, Velayutham E (2021) Is industrial pollution detrimental to public health? Evidence from the world's most industrialized countries. BMC Public Health 21:1175. https://doi.org/10.1186/s12889-021-11217-6

Ramírez-Pérez AM, Álvarez-Vázquez MA, de Uña-Álvarez E, de Blas E (2020) Environmental assessment of trace metals in San Simón Bay sediments NW Iberian Peninsula. Minerals 10:826. https://doi.org/10.3390/min10090826

Reimann C, de Caritat P (2000) Intrinsic flaws of element enrichment factors EFs in environmental geochemistry. Environ Sci Technol 34:5084–5091

Ribeiro A, Pereira E, Dias R (1990) Structure in the northwest of the Iberian Peninsula. In: Dallmeyer RD, Martínez Garcia E (eds) Pre-Mesozoic Geology of Iberia. Springer-Verlag, Berlin, Heidelberg, pp 220–236

Ribeiro S, Amorim A, Abrantes F, Ellegaard M (2016) Environmental change in the Western Iberia Upwelling Ecosystem since the preindustrial period revealed by dinoflagellate cyst records.

The Holocene 2016(266):874–889. https://doi.org/10.1177/0959683615622548
Ribeiro S, Santos JF, Martins V, Soares AS, Castro N (2011) Procedures for Sr and Nd isotope analysis in the terrigenous component of marine sediments. VIII Congresso Ibérico de Geoquímica/XVII Semana de Geoquímica, VIII CIG/XVI-ISG, Escola Superior Agrária, Instituto Politécnico de Castelo Branco, 24 e 28 de Setembro de 2011. http://hdl.handle.net/10773/9052
Renberg I, Bindler R & Brännvall ML (2001) Using the historical atmospheric leaddeposition record as a chronological marker in sediment deposits in Europe. The Holocene 11(5):511–516
Ríos A, Nombela MA, Pérez F, Rosón G, Fraga F (1992) Calculation of runoff to an estuary. Ria De Vigo Sci Mar 561:29–33
Rodrigues J, Pereira E, Ribeiro A (2013) Complexo de mantos parautóctones do NE de Portugal: estrutura interna e tectonoestratigrafia. In: Geologia de Portugal R. Dias, A. Araújo, P. Terrinha and J. Kullberg Eds.. Escolar Editora, pp. 275–332.
Rodríguez Pérez JA (1985) A minaria do volfrámio em galiza 1887–1960. Umha Primeira Aproximaçom Agália 2:49–70
Rodríguez-Racedo J, García-Rodeja E, Martínez-Cortizas A (2013) Five thousand years of atmospheric Ni, Zn, As, and Cd deposition recorded in bogs from NW Iberia: prehistoric and historic anthropogenic contributions. J Archaeol Sci 40:764–777
Roos-Barraclough F, Martínez Cortizas A, García-Rodeja E, Shotyk W (2002) A 14,500 year record of the accumulation of atmospheric mercury in peat: volcanic signals, anthropogenic influences and a correlation to bromine accumulation, Earth Planet. Sci Lett 202:435–451
Rosman KJR, Chisholm W, Hong S, Candelone JP, Boutron CF (1997) Lead from Carthaginian and Roman Spanish mines isotopically identified in Greenland ice dated from 600 BC to 300 AD. Environ Sci Technol 31:3413–3416
Rovira S (2002) Metallurgy and Society in Prehistoric Spain. In Ottaway, B. S., and Wager, E. eds., Metals and Society. Papers from a Session Held at the European Association of Archaeologists Sixth Annual Meeting in Lisbon 2000, 5–20. BAR-IS1061. London: Archaeopress.
Rubio B, Nombela MA, Vilas F (2000) Geochemistry of major and trace elements in sediments of the Ria de Vigo NW Spain: an assessment of metal pollution. Mar Pollut Bull 40(11):968–980
Rubio B, Álvarez-Iglesias P, Vilas F (2010) Diagenesis and anthropogenesis of metals in the recent Holocene sedimentary record of the Ria de Vigo N.W. Spain Marine Pollution Bulletin 60:1122–1129
Sanchez Pardo JC (2013) Power and rural landscapes in early medieval Galicia 400–900 ad: towards a re-incorporation of the archaeology into the historical narrative. Early Medieval Europe 21(2):140–168
Santos Zalduegui JF, Schgrer U, Gil Ibarguchi JI (1995) Isotope constraints on the age and origin of magmatism and metamorphism in the Malpica-Tuy allochthon, Galicia, NW Spain. Chem Geol 121:91–103
Santos Zalduegui JF, Schärar U, Gil Ibarguchi JI, Girardeau J (1996) Origin and evolution of the Paleozoic Cabo Ortega ultramafic-mafic complex NW Spain: U-Pb, Rb-Sr and Pb-Pb isotope data. Chem Geol 129:281–304
Schulz HD, Zabel M (2006) Marine Geochemistry, 2nd edn. Springer, Germany, p 582
Shannon CE (1948) A mathematical theory of communication. Bell Systems Technological Journal 27:379–423
Silva TR, Lopes SRP, Spörl G, Knoppers BA, Azevedo DA (2012) Source characterization using molecular distribution and stable carbon isotopic composition of n–alkanes in sediment cores from the tropical Mundaú-Manguaba estuarine–lagoon system, Brazil. Org Geochem 53:25–33
Silva-Sánchez N, Martínez Cortizas A, López-Merino L (2014) Linking forest cover, soil erosion and mire hydrology to late-Holocene human activity and climate in NW Spain. The Holocene 24:714–725. https://doi.org/10.1177/0959683614526934
Snoeckx H, Grousset FE, Revel M, Boelaert A (1999) European contribution of ice-rafted sand to Heinrich layers H3 and H4. Mar Geol 158:197–208
Soares AMM, Dias JMA (2007) Reservoir effect of coastal waters off Western and Northwestern Galicia. Radiocarbon 49(2):925–936
Sutherland RA (2000) Bed sediment–associated trace metals in an urban stream, Oahu. Hawaii Environmental Geology 39:611–627. https://doi.org/10.1007/s002540050473
Swindles GT, Watson EJ, Savov IP, Lawson IT, Schmidt A, Hooper A, Cooper CL, Connor CB, Gloor M, Carrivick JL (2018) Climatic control on Icelandic volcanic activity during the mid-Holocene. Geology 46(1):47–50. https://doi.org/10.1130/G39633.1
Taylor S (1964) Abundance of chemical elements in the continental crust: A new table. Geochim Cosmochim Acta 28:1273–1285
Taylor SR, Mclennan SM (1985) The Continental Crust: Its Composition and Evolution. Blackwell Scientific Publications, Hoboken, NJ, USA, p 312
Thordarson T, Höskuldsson A (2008) Postglacial volcanism in Iceland. Jökull 58:197–228
Tornos F, Ribera F, Shepherd TJ, Spiro B (1996) The geological and metallogenic setting of stratabound carbonate hosted Zn–Pb mineralizations in the West Asturian Leonese Zone, NW Spain. Miner Depos 31:27–40
Torres R, Barton ED (2007) Onset of the Iberian upwelling along the Galician coast. Cont Shelf Res 27:1759–1778
Troen I, Petersen EL (1989) European Wind Atlas. Riso National Laboratory: Roskilde, Denmark, p. 656.
Turekian KK, Wedepohl KH (1961) Distribution of the elements in some major units of the Earth's crust. Geol Soc Am Bull 72:175–192
Urbano R, Toyos M, Asensio B (1998) Intragranitic lode gold deposits in the Tomiño area Pontevedra. Cuaderno Lab Xeolóxico De Laxe Coruña 17:341–348
Velasco F, Pesquera A, Herrero JM (1996) Lead isotope study of Zn–Pb ore deposits associated with the Basque-Cantabrian basin and Paleozoic basement, Northern Spain. Miner Depos 31:84–92
Vilas F, Nombela MA, García-Gil E, García-Gil S, Alejo I, Rubio B, Pazos Ó (1995) Cartografia de sedimentos submarinos de la Ría de Vigo. Xunta de Galicia. Consellería de Pesca, Marisqueo e Acuicultura, 40 pp.
Vilas F, Bernabeu A, Rubio B, Rey D (2019) The Galician Rias. NW Coast of Spain. In: Morales, J. A. Ed. The Spanish coastal systems. Dynamic processes, sediments and management. Springer-Nature Switzerland AG 2019, Chapter 17, pp 387–414. https://doi.org/10.1007/978-3-319-93169-2_17
Vitorino J, Oliveira A, Jouanneau JM, Drago T (2002) Winter dynamics on the northern Portuguese shelf: Part 1. Physical Processes Prog Oceanogr 52(2–4):129–153
Von Knorring O, Vidal Romani JR (1981) On the mineralogy of the O Casteliño spodumene pegmatite near Lalin, Galicia, Spain Cadernos do Laboratorio Xeolóxico de Laxe, 2.2, 259–262. http://hdl.handle.net/2183/5779
Weeks L (2003) Early Metallurgy of the Persian Gulf: technology, trade and the Bronze Age. World. Boston: Brill
Wheeler DL (1986) The Price of Neutrality: Portugal, the Wolfram Question, and World War II. Luso-Brazilian Review 23 1, pp. 107–127. Published By: University of Wisconsin Press. https://www.jstor.org/stable/3513391
Windom HL, Schropp SJ, Calder FD, Ryan JD, Smith RG Jr, Burney LC, Lewis FG, Rawlison CH (1989) Natural trace metal concentration in estuarine and coastal marine sediments of the Southeastern United States. Environ Sci Technol 233:314–320

Wollast R (1998) The global coastal zone, processes and methods. In The Sea Brink, K. H. & Robinson, A. R., eds, John Wiley & Sons, New York, pp. 213–252.

Wooster W et al (1976) Seasonal upwelling cycle along the eastern boundary of the North Atlantic. J Mar Res 34:131–140

Yano M, Yasukawa K, Nakamura K, Ikehara M, Kato Y (2020) Geochemical features of redox-sensitive trace metals in sediments under oxygen-depleted marine environments. Minerals 10:1021. https://doi.org/10.3390/min10111021

Zalasiewicz J, Williams M, Haywood A, Ellis M (2011) The Anthropocene: a new epoch of geological time? Phil Trans R Soc A 369:835–841. https://doi.org/10.1098/rsta.2010.0339